Larsen, H.C., Duncan, R.A., Allan, J.F., Brooks, K. (Eds.), 1999
Proceedings of the Ocean Drilling Program, Scientific Results, Vol. 163

8. Sr, Nd, AND Pb ISOTOPES AND TRACE ELEMENT GEOCHEMISTRY OF BASALTS FROM THE SOUTHEAST GREENLAND MARGIN[1]

Andrew D. Saunders,[2] Pamela D. Kempton,[3] J. Godfrey Fitton,[4] and Lotte Melchior Larsen[5]

ABSTRACT

Voluminous, subaerial magmatism resulted in the formation of extensive seaward-dipping reflector sequences (SDRS) along the Paleogene Southeast Greenland rifted margin. Drilling during Leg 163 recovered basalts from the SDRS at 66°N (Site 988) and 63°N (Sites 989 and 990). The basalt from Site 988 is light rare-earth-element (REE) enriched (La_n/Yb_n = 3.4), with $\varepsilon Nd_{(t=60)}$ = 5.3, $^{87}Sr/^{86}Sr$ = 0.7034, and $^{206}Pb/^{204}Pb$ = 17.98. It is similar to tholeiites recovered from the Irminger Basin during Leg 49 and to light-REE–enriched tholeiites from Iceland. Drilling at Site 989, the innermost of the sites on the 63°N transect, was proposed to extend recovery of the earliest part of the SDRS initiated during Leg 152. These basalts are, however, younger than those from Site 917 and are compositionally similar to basalts from the more seaward Sites 990 and 915. Many of the basalts from Sites 989 and 990 show evidence of contamination by continental crust (e.g., $\varepsilon Nd_{(t=60)}$ extends down to –3.7, $^{206}Pb/^{204}Pb$ extends down to 15.1). We suggest that the contaminant is a mixture of Archean granulite and amphibolite and that the most contaminated basalts have assimilated ~5% of crust. Uncontaminated basalts are isotopically similar to basalts from Site 918, on the main body of the SDRS, and are light-REE depleted. Consistent with previous models of the development of this margin, we show that at the time of formation of the basalts from Sites 989 and 990 (1) melting was at relatively shallow levels in a fully fledged rift zone; (2) fragments of continental crust were present in the lithosphere above the zones of melt generation; and (3) the sublithospheric mantle was dominated by a depleted Icelandic plume component.

INTRODUCTION

In this paper we present new isotope (Sr, Nd, and Pb) and complementary whole-rock major and trace element data for a suite of basalts recovered from Sites 988, 989, and 990. All three sites are located on the seaward-dipping reflector sequences (SDRS) of the Southeast Greenland rifted margin (Duncan, Larsen, Allan, et al., 1996), a region of intense volcanic activity during the late Paleocene and Eocene (Larsen and Jakobsdóttir, 1988; Sinton and Duncan, 1998; Tegner and Duncan, Chap. 6, this volume). The data complement the geochemical study of a larger sample set presented by Larsen et al. (Chap. 7, this volume).

A major goal of Leg 163 was to retrieve lavas from the Paleogene SDRS and compare them with lavas recovered during Leg 152 (Larsen, Saunders, Clift, et al., 1994). Specifically, Site 988 at latitude 66°N was aimed at characterizing lavas erupted closer to the axis of the ancestral Iceland plume (Fig. 1). Sites 989 and 990, both located on a transect at 63°N, were aimed at extending and interpolating the recovery achieved during Leg 152. Because of operational and weather difficulties, Leg 163 achieved only limited success, but did recover a total of about 196 m of basalt. The bulk of the core came from Hole 990A. We begin by summarizing the results of Leg 152.

SUMMARY OF LEG 152 RESULTS

Scientists on Leg 152 visited the Southeast Greenland margin during 1993. Of the six sites on the 63°N transect, drilling at three of these (Sites 915, 917, and 918) recovered material from the SDRS (Figs. 1, 2) (Larsen, Saunders, Clift, et al., 1994). Hole 917A was the most successful, penetrating 779 m through the lava pile into an underlying sequence of steeply inclined metasediments. The succession at Site 917A, comprising 91 flow units (as defined in Larsen, Saunders, Clift, et al., 1994), has been divided into an Upper, Middle, and Lower Series on the basis of shipboard and subsequent shore-based mineralogical and geochemical studies (see Demant, 1998; Fitton et al., 1998a, 1998b; Fram et al., 1998; L.M. Larsen et al., 1998). Both the Lower and Middle Series are strongly contaminated by continental crust of various types (Fitton et al., 1998a) (see below), but the extent of contamination decreases dramatically in the succeeding Upper Series. The Upper Series, which is separated from the Middle Series by a sediment horizon, is characterized by picritic and high-Mg basalts and, although many of these lavas may be olivine accumulative, some represent true high-Mg liquids (Thy et al., 1998). The basalts of the Lower and Upper Series were derived mainly from a sublithospheric source with a predominantly mid-ocean-ridge basalt (MORB)-like composition, but several units close to the top of the Lower Series have Icelandic affinities (Fitton et al., 1998a, 1998b).

Site 915, located 3 km to the southeast of 917, recovered material from three igneous units higher in the SDRS lava pile. The basalt from Site 915 shows evidence of slight contamination of the parental magma by continental crust, but the MgO content is normal (7.5%), indicating that the phase of picritic magmatism recorded at Site 917 had, by this time, ceased. Basalts from Site 918 on the main sequence of the SDRS are uncontaminated, erupted in a subaerial environment through crust with no continental component. Unit 918-1 may be a sill, emplaced into the overlying Eocene sediments. For convenience, the lavas from the Lower and Middle Series from Site 917 have been

[1]Larsen, H.C., Duncan, R.A., Allan, J.F., Brooks, K. (Eds.), 1999. *Proc. ODP, Sci. Results*, 163: College Station, TX (Ocean Drilling Program).
[2]Department of Geology, University of Leicester, Leicester, LE1 7RH, United Kingdom. ADS@LE.AC.UK
[3]NERC Isotope Geoscience Laboratories, Keyworth, Nottingham, NG12 5GG, United Kingdom.
[4]Department of Geology and Geophysics, Grant Institute, University of Edinburgh, West Mains Road, Edinburgh, EH9 3JW, United Kingdom.
[5]Danish Lithosphere Centre, Øster Voldgade 10, L, 1350 Copenhagen K, Denmark.

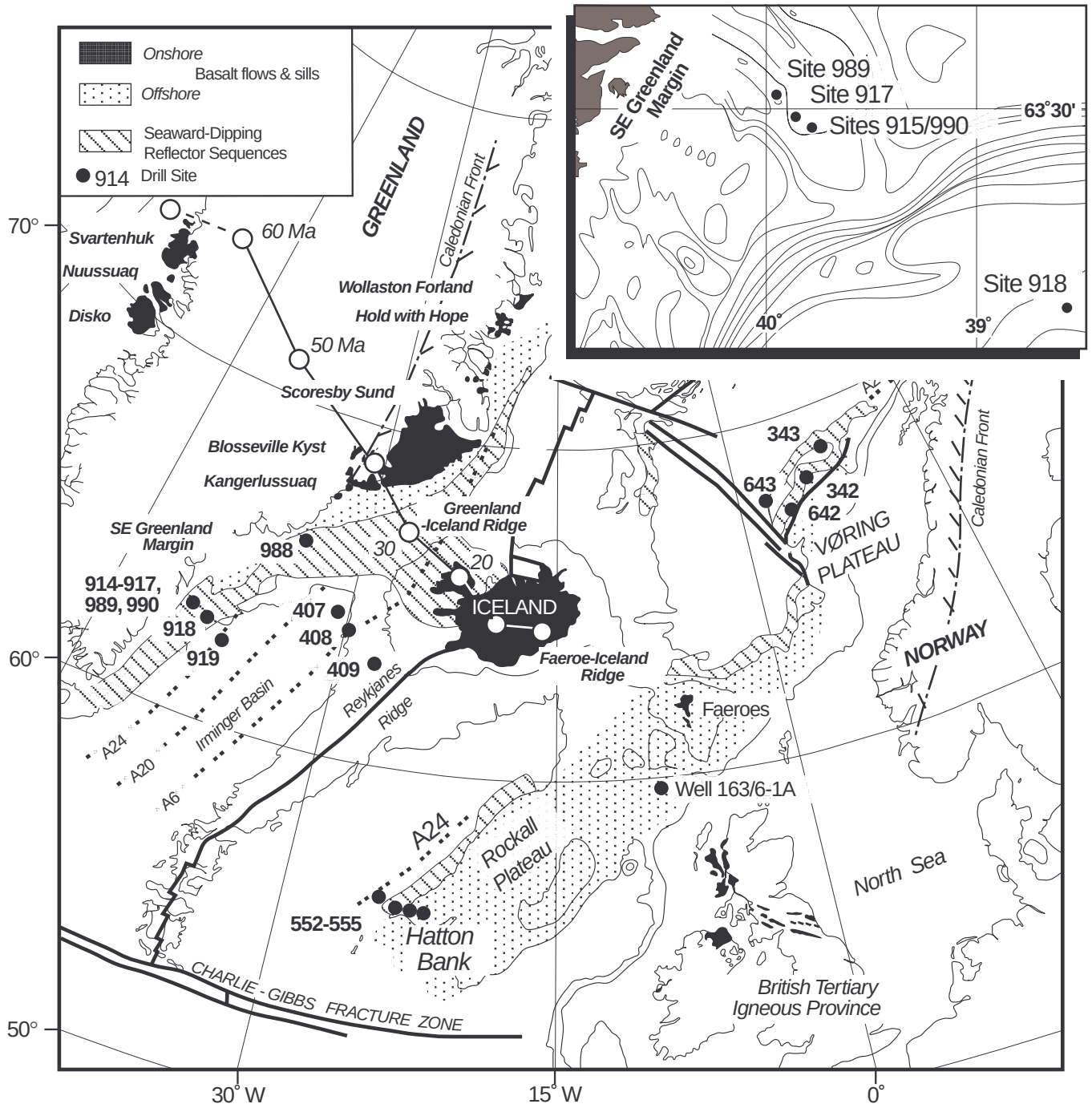

Figure 1. Map of the North Atlantic region showing the main physiographic features and the main drill sites mentioned in this paper. Modified after Larsen, Saunders, Clift et al. (1994). Open circles = locations of Iceland hotspots from 60 Ma from Lawver and Müller (1994). Inset shows locations of drill sites on Southeast Greenland margin.

termed the "continental succession," whereas those from the Upper Series, and from Sites 915 and 918, have been termed the "oceanic succession" (e.g., Larsen and Saunders, 1998). It is, however, important to stress that at least the earlier parts of the oceanic succession (basalts from 917 Upper Series and Site 915) do show some evidence of contamination by continental crust. The lavas from Sites 915 and 918 show affinities with depleted Icelandic basalts (Fitton et al., 1998a, 1998b).

Radiometric dating of the Leg 152 material (Sinton and Duncan, 1998) shows that the continental succession was erupted at ~60–61 Ma (Chron C26r or 27r), which is substantially earlier than was originally thought (Chron C24r). No dates are available for the lavas from the Upper Series at Sites 917, 915, or 918, but the lavas at Site 918 are ~54 m.y. old on the basis of a dated late basalt unit and their magnetic polarity (Larsen and Saunders, 1998). The Site 917 Upper Series picrites and basalts appear to have been emplaced during a period of significant lithospheric thinning, as evidenced by the dramatic decrease in Sm/Lu and Zr/Sc ratios indicative of a reduction in the average pressure of melt segregation (Fram et al., 1998; Saunders et al., 1998; see also Larsen et al., Chap. 7, this volume).

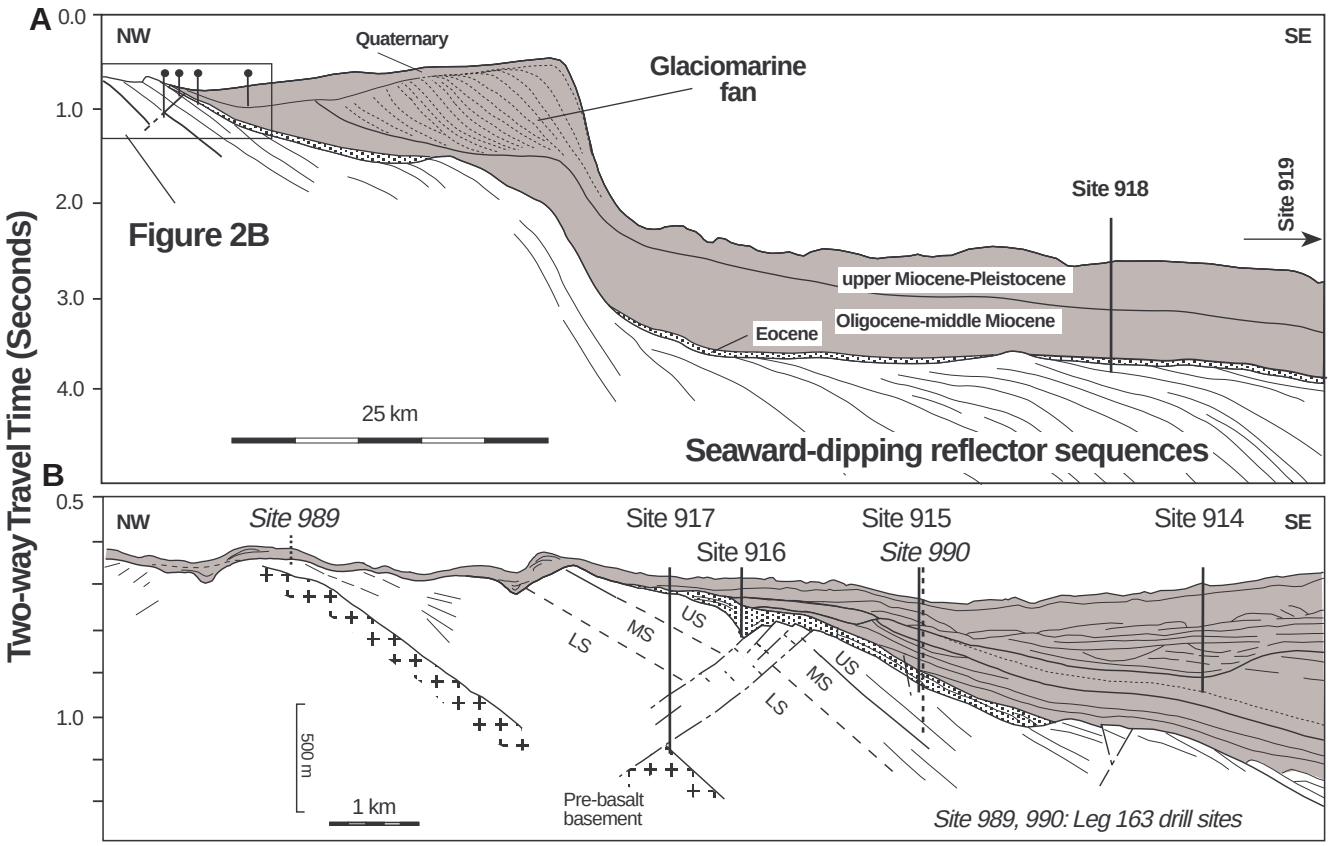

Figure 2. **A.** Section across the Southeast Greenland margin at latitude 63°N, showing the locations of the holes drilled during Legs 152 and 163. Site 919, which lies to the east, and Site 988, which lies to the north, are not shown. **B.** Expansion of the featheredge of the SDRS. Modified after Larsen, Saunders, Clift et al. (1994) and Duncan, Larsen, Allan, et al. (1996).

From Leg 152, a picture has emerged of an evolving volcanic rifted margin somewhat different than anticipated before that leg commenced. The earlier continental succession, emplaced at 60–61 Ma, is coeval with activity in west Greenland and the British Tertiary Igneous Province (see review by Saunders et al., 1997). This activity preceded the main episode of continental rupture, but followed prolonged basin development during the Cretaceous. The tilted metasediments recovered from the bottom of Hole 917D were probably deposited in one of these precursor basins, but the sediments remain undated. Full-scale continental rupture occurred after the Middle Series was emplaced, probably during the eruption of the Upper Series magmas, but possibly later. However, the lack of dates for any of the post-Middle Series lavas makes further refinement of the tectonic events speculative.

The significance of Leg 163 drilling to our understanding of the 63°N transect thus becomes apparent. Drilling at Site 989, the most westerly site on the transect, was planned to penetrate the oldest part of the featheredge of the SDRS and into the underlying basement, thus allowing us to characterize the oldest lavas, the unconformity, and the basement. Site 990, close to Site 915, was planned to extend the Site 915 drilling to a depth where, ideally, picritic lavas similar to those recovered from Site 917 would be recovered (see Fig. 2), thus providing a more or less continuous recovery across a critical interval in the SDRS.

Site 988 is located on SDRS that were erupted closer to the proposed ancestral Iceland plume and basalts from this site should, therefore, have a clear Icelandic signature. This site is also at the western end of a previous transect of holes drilled in the Irminger Basin during Leg 49 (Luyendyk, Cann, et al., 1979). Basalts from Holes 407, 408, and 409 are distinct from MORB and more closely resemble basalts recovered from the Reykjanes Ridge north of 61°N (e.g., Tarney et al., 1979; Wood et al., 1979).

The new data presented here demonstrate that the majority of the basalts recovered at Sites 989 and 990 are contaminated by continental crust, which is consistent with their eruption site close to, and probably landward of, the continent-ocean transition (H.C. Larsen et al., 1998). They have not suffered the same amount of contamination as many of the Lower and Middle Series basalts recovered at Site 917 (Fitton, et al., 1998a, 1998b), or the Lower Series lavas at Site 642 on the Vøring Plateau (e.g., Viereck et al., 1988, 1989), where peraluminous dacites are found. They do, however, provide additional evidence that many lavas associated with North Atlantic SDRS were contaminated during ascent to the surface, with concomitant implications for understanding the subsidence histories of the margins and deciphering the composition of the mantle source regions.

SUMMARY OF LITHOLOGY, PETROLOGY, AND SECONDARY ALTERATION

Site 988

Hole 988A is located at ~66°N, ~56 km offshore of the Southeast Greenland coast in 262.6 m of water, where the upper part of the lava sequence, as identified by seismic profiles, crops out at the seabed. Two basaltic flow units were recognized in the core (Duncan, Larsen, Allan, et al., 1996). Unit 988-1 is a dark-greenish-gray plagioclase-pyroxene-olivine-phyric basalt, between 19 and 21 m thick. The unit has a massive aspect and is sparsely vesicular; the vesicles are mostly filled with smectite/saponite, although some contain chabazite. The glassy groundmass and the majority of the sparse olivine phenocrysts

have been replaced by smectite. Unit 988-2, of which only 98 cm were recovered, is, by contrast, highly altered. It appears to be the scoriacious, oxidized top of a basaltic flow that was erupted in a subaerial environment.

Site 989

Site 989 is located 43 km offshore of the east Greenland coast at 63°N on the extreme western featheredge of the SDRS. Drilling at this site was planned to extend the transect drilled during Leg 152, in particular to drill through the SDRS and determine the nature of both the pre-eruptive unconformity and the underlying basement. From the seismic profiles, it was predicted that the basalt at this site would be older than that recovered at Site 917, but the relative freshness of the material and the subsequent Ar-Ar studies show that the basalts were emplaced at about 56 Ma, some 4 m.y. after the Lower and Middle Series from Site 917 (Tegner and Duncan, Chap. 6, this volume). Weather conditions terminated the drilling at this site after 84.2 m of penetration in Hole 989B, long before sub-basaltic basement was reached. Hole 989A reached 21.4 m below seafloor (mbsf) and recovered basalt similar to that from the upper part of Hole 989B.

Two igneous units were identified in the core from Hole 989B (Duncan, Larsen, Allan, et al., 1996). Unit 1 is a gray, vesicular, moderately altered, aphyric basalt and is at least 69 m thick. The unit contains 69 repeated bands with textural variations (especially vesicle size and content) interpreted by the shipboard party as the more rapidly cooled tops of pahoehoe flow lobes. Unit 2 was cored from 73.2 mbsf to the bottom of the hole, so it is at least 11 m thick.

Unit 1 contains rare plagioclase glomerocrysts, with a groundmass comprising plagioclase, augite, magnetite, trace amounts of olivine, and up to 15% mesostasis. Both the mesostasis and the olivine are completely replaced by clay. Vesicles are open or filled by smectite, zeolites, calcium carbonate, and minor pyrite, and veins of secondary minerals are present throughout the unit. Unit 2 is slightly to moderately porphyritic with phenocrysts of plagioclase (2%–3%), augite (1%–2%), and olivine (trace to 2%) in a microcrystalline groundmass. Again, the groundmass and the olivine are completely replaced by clay. Shipboard X-ray diffraction studies show that the replacement clays in both units are predominantly saponite-dominated smectite-illite mixed-layer clays. Vesicles are commonly lined with smectitic clay and, near veins, zeolite (stilbite, clinoptilolite, and heulandite).

The top of neither unit was recovered in the drill core, so the environment of eruption is unknown; the nature of the pahoehoe subunits in Unit 1 suggests, however, that this unit was erupted subaerially. The secondary mineral assemblages are similar to those reported for subaerial flows from Iceland and the Faeroes, but the possibility of subaqueous eruption cannot be precluded (Duncan, Larsen, Allan, et al., 1996; Teagle and Alt, Chap. 13, this volume).

Site 990

Site 990 is located 52 km east of the Southeast Greenland coast, close to the previous Site 915. That earlier site achieved only limited recovery of an important section of the SDRS, which subsequently proved to be undateable by Ar-Ar methods (Sinton and Duncan, 1998). Recovery at Site 990 was more successful. The first igneous unit was in Section 163-990A-5R-1 at 211.9 mbsf, and 13 units were recognized before the hole was terminated at 342.7 mbsf. Unfortunately, the hole was terminated before we could demonstrate lithologic contiguity with the Upper Series at Site 917, a major goal of Site 990.

The shipboard party recognizes three flow types within the core, interpreted as being aa (Units 990-1 to -3 and possibly -13), pahoehoe (Units 990-8 to -12) and transitional aa-pahoehoe types (Units 990-4 to -7). The aa flows characteristically have thicker brecciated tops, are thicker overall than the pahoehoe flows, and are at the top of the drilled succession. A vein or dike of basalt was recovered within Unit 990-12 in Sample 163-990A-24R-1 (Piece 3, 15–22 cm) and will be considered as a separate unit (dike). The top of the volcanic sequence at Sites 990 and 915 is deeply weathered and oxidized, and all of the lava flow units have oxidized flow tops. Some units are separated by thin layers of red soil. Eruption, therefore, probably occurred under subaerial conditions.

The flow units cored at Site 990 range from aphyric to highly olivine or plagioclase-olivine-clinopyroxene phyric basalt (see Duncan, Larsen, Allan, et al., 1996; a summary is included in Table 1). Most units are moderately porphyritic, with both plagioclase and olivine phenocrysts, although Units 6, 7, and 9 comprise aphyric olivine basalts. The gray flow interiors sampled for this study are moderately altered, in contrast to the highly or completely altered flow tops. Olivine and mesostasis are completely recrystallized to green smectite clays. Vesicle content varies strongly according to location of samples in the different types of flow units. Vesicles are generally lined or partly to completely filled by clay minerals. Zeolite-filled vesicles, and carbonate-bearing cavities, are much less abundant in the flow interiors than in the oxidized flow tops. Zeolites found in the Site 990 lavas include phillipsite, chabazite, and clinoptilolite. Native copper is a ubiquitous phase in these basalts, found in veins associated with green clays and in some vesicles.

ANALYTICAL METHODS

Samples were taken from the least altered portions of all of the lithologic units identified by the shipboard party (Duncan, Larsen, Allan, et al., 1996), washed, dried, and crushed in an agate Tema swingmill at the University of Edinburgh. Aliquots of powder were analyzed for major (by Larsen at Copenhagen) and trace (by Fitton at Edinburgh) elements by X-ray fluorescence (XRF); a subset of the samples was sent to Leicester (Saunders) for determination of the rare earth elements (REEs), Co, Sc, Th, Ta, and Hf by instrumental neutron activation analysis (INAA); and to the NERC Isotope Geosciences Laboratories (Kempton) for isotopic analysis. The subsets of data are presented in Tables 1 and 2; data for international and shipboard reference standards are given in Table 3. Major and trace element data for the complete set of samples are presented by Larsen et al. (Chap. 7, this volume). Full details of the XRF analytical techniques used at Edinburgh and Copenhagen are published in Fitton et al. (1998b) and Larsen et al. (Chap. 7, this volume), respectively; details of INAA techniques are given in Fitton et al. (1998b). Full ODP designation for each sample is included in Tables 1 and 2.

Sr, Nd, and Pb isotope ratios were determined at the NERC Isotope Geosciences Laboratories. Samples were leached in 2 ml 6M HCl on a hot plate at ~100°C for ~60 min before dissolution. The leachates were removed and the residue rinsed in Milli-Q (reverse osmosis, deionized) H_2O. The leachates and the final Milli-Q H_2O rinses were combined and processed for isotopic analysis. One unleached whole rock powder from Unit 990-13 was also analyzed to compare with leached residue results. Sr, Nd, and Pb were run as the metal species on single Ta, double Ta-Re, and single Re filaments, respectively. Nd and Pb were analyzed using a Finnigan MAT 262 multicollector mass spectrometer in static mode; Sr was run on a VG354 multicollector mass spectrometer in dynamic mode. Blanks for Sr, Nd, and Pb during the course of analysis were <1 ng, 100 pg, and 700 pg, respectively. $^{87}Sr/^{86}Sr$ was normalized during the run to a value of $^{86}Sr/^{84}Sr = 0.1194$; $^{143}Nd/^{144}Nd$ was similarly normalized to a value of $^{146}Nd/^{144}Nd = 0.7219$. Sample values are reported relative to accepted values for NBS987 and J&M of 0.71024 and 0.51111, respectively. Minimum uncertainties are derived from external precision (1 stan-

Table 1. Major and trace element data for selected Leg 163 samples.

Sample	988A-4R-1 (Piece 11, 92-98 cm)	989B-10R-2 (Piece 2, 9-15 cm)	989B-11R-1 (Piece 7, 58-63 cm)	990A-9R-3 (Piece 3C, 76-82 cm)	990A-13R-3 (Piece 9A, 97-103 cm)	990A-18R-6 (Piece 3A, 76-82 cm)	990A-22R-1 (Piece 4, 47-53 cm)	990A-23R-2 (Piece 2B, 41-47 cm)	990A-24R-1 (Piece 3, 15-18 cm)	990A-24R-3 (Piece 2A, 16-10 cm)
Depth (mbsf)	27.92	65.92	74.68	244.33	263.9	296.1	318.37	329.17	337.25	340.03
Unit	988-1	989-1	989-2	990-2	990-3A	990-6	990-10	990-11	990 dike	990-13
Phenocrysts	Pl, aug, ol	Aphyric	Pl	Pl, (ol)	Pl, ol, (aug)	(Pl, aug)	Aphyric	Pl, ol, (aug)	Aphyric	Pl, (ol)
Major oxides (wt%; X-ray fluorescence analysis by Copenhagen)										
SiO_2	48.83	49.91	50.43	50.88	49.40	50.33	50.23	50.98	49.57	50.58
TiO_2	2.442	1.006	0.914	0.964	0.938	0.968	0.751	0.777	1.757	0.799
Al_2O_3	14.00	13.71	14.17	15.33	15.02	14.29	16.00	15.99	14.64	14.04
Fe_2O_3	4.22	5.39	2.64	2.89	6.21	2.89	4.41	5.25	4.91	4.39
FeO	8.80	7.29	8.71	8.06	5.84	7.71	5.70	4.80	7.02	6.76
MnO	0.21	0.20	0.21	0.19	0.21	0.22	0.17	0.17	0.20	0.19
MgO	6.12	7.94	7.87	6.83	7.19	8.02	7.14	6.67	6.02	7.84
CaO	11.26	11.20	12.39	11.58	11.65	12.10	11.22	11.52	10.84	11.13
Na_2O	2.63	2.05	1.95	2.16	2.15	1.98	1.93	2.09	2.36	1.86
K_2O	0.33	0.06	0.10	0.19	0.19	0.11	0.16	0.22	0.29	0.25
P_2O_5	0.28	0.09	0.09	0.10	0.09	0.10	0.08	0.09	0.16	0.06
Volatiles	0.84	1.34	0.77	0.94	1.18	1.13	2.10	1.56	1.52	2.15
Total	99.97	100.18	100.24	100.09	100.06	99.85	99.90	100.13	99.29	100.07
Trace elements (ppm; X-ray fluorescence analysis by Edinburgh)										
Nb	17.8	1.9	2.2	2.1	2.0	2.7	1.7	1.4	3.1	1.2
Zr	165	45	47	57	53	49	41	42	102	39
Y	37	24	24	25	26	23	18	21	37	20
Sr	242	69	84	119	90	107	88	96	112	71
Rb	3	1	2	2	3	1	3	2	3	4
Th	2.0	0.7	0.6	0.3	1.2	0.6	0.5	0.5	1.1	0.6
Pb	3.4	0.3	0.2	1.8	0.7	1.1	0.2	0.6	0.7	bdl
La	15	5	2	5	3	5	4	2	4	bdl
Ce	39	7	10	12	9	8	9	10	13	8
Nd	27	4	7	7	7	7	6	6	12	4
Zn	108	88	85	85	87	83	68	71	121	84
Cu	206	195	151	115	91	107	57	78	252	56
Ni	71	80	96	72	77	96	108	83	72	104
Co	61	56	51	46	48	48	44	43	47	50
Cr	128	54	219	129	132	212	249	229	98	247
V	380	409	328	309	332	322	253	257	471	301
Ba	125	19	34	69	34	57	26	80	10	18
Sc	38	52	51	46	49	52	41	43	65	51
Ga	22	16	16	16	16	16	16	17	20	15
Trace elements (ppm; neutron activation analysis by Leicester)										
La	15.0	1.9	2.2	4.0	3.3	3.5	2.7	2.8	3.7	1.7
Ce	33.3	4.5	6.2	10.6	7.4	8.1	6.3	6.4	10.7	4.4
Nd	21.0	3.7	4.6	8.1	6.0	6.0	4.2	5.1	10.5	3.8
Sm	5.53	1.75	1.87	2.11	2.1	1.99	1.57	1.66	3.7	1.53
Eu	1.91	0.71	0.81	0.88	0.81	0.83	0.62	0.71	1.45	0.64
Gd	6.22	2.73	2.74	3.02	3.32	2.91	2.62	2.62	5.78	2.29
Tb	1.01	0.6	0.59	0.59	0.62	0.61	0.45	0.53	0.97	0.48
Yb	3.02	2.42	2.47	2.41	2.57	2.31	1.87	2.07	3.33	2.04
Lu	0.45	0.34	0.45	0.39	0.39	0.39	0.31	0.34	0.52	0.32
Ta	0.98	0.11	0.13	0.13	0.1	0.15	0.07	0.08	0.16	0.08
Th	1.31	0.24	0.22	0.33	0.37	0.27	0.23	0.22	0.26	0.14
Hf	4.22	1.27	1.49	1.61	1.45	1.42	1.11	1.23	2.77	1.17
Sc	40.8	54.7	51.2	45.7	50.2	51.5	43.3	44.9	55.4	49.9
Co	50.2	62.2	50.8	50.5	56.2	51.0	46.7	44.3	49.0	48.5
U	bdl	bdl	bdl	bdl	bdl	bdl	bdl	bdl	bdl	bdl

Notes: Phenocrysts: pl = plagioclase; ol = olivine; aug = augite. () = <1%. bdl = below detection level.

Table 2. Isotope data for selected Leg 163 samples.

Sample	988A-4R-1 (Piece 11, 92-98 cm)	988A-10R-2 (Piece 2, 9-15 cm)	989B-11R-1 (Piece 7, 58-63 cm)	990A-9R-3 (Piece 3C, 76-82 cm)	990A-13R-3 (Piece 9A, 97-103 cm)	990A-18R-6 (Piece 3A, 76-82 cm)	990A-22R-1 (Piece 4, 47-53 cm)	990A-23R-2 (Piece 2B, 41-47 cm)	990A-24R-1 (Piece 3, 15-18 cm)	990A-24R-3 (Piece 2A, 16-10 cm)	990A-24R-3 (Piece 2A, 16-10 cm)
Depth (mbsf)	27.92	65.92	74.68	244.33	263.9	296.10	318.37	329.17	337.25	340.03	340.03
Unit	988-1	989-1	989-2	990-2	990-3A	990-6	990-10	990-11	990 dike	990-13	990-13 (u)
Nd (ppm)	21.0	3.7	4.6	8.1	6.0	6.0	4.2	5.1	10.5	3.8	
Sm (ppm)	5.53	1.75	1.87	2.11	2.10	1.99	1.57	1.66	3.70	1.53	
$^{147}Sm/^{144}Nd$	0.166	0.294	0.253	0.163	0.218	0.209	0.235	0.205	0.220	0.255	0.255
$^{143}Nd/^{144}Nd_m$	0.512896	0.513129	0.512908	0.512437	0.512697	0.512700	0.512621	0.512644	0.513134	0.512911	0.512889
$\varepsilon Nd_{(t=60)}$	5.27	8.84	4.83	-3.67	0.99	1.12	-0.62	0.05	9.50	4.88	4.45
$^{87}Sr/^{86}Sr_m$	0.703350	0.702975	0.703508	0.703332	0.704366	0.703861	0.703526	0.703520	0.702884	0.703494	0.704039
$^{206}Pb/^{204}Pb_m$	17.981	18.100	16.846	15.179	15.816	16.301	15.907	15.709	18.029	16.888	16.931
$^{207}Pb/^{204}Pb_m$	15.414	15.459	15.163	14.750	14.905	14.995	14.948	14.866	15.407	15.177	15.174
$^{208}Pb/^{204}Pb_m$	37.884	37.834	37.191	35.495	37.254	36.914	36.296	36.109	37.753	37.321	37.286

Note: Subscript m = measured ratios; (u) = unleached sample.

dard deviation) of standard measurements that average 14 ppm for $^{143}Nd/^{144}Nd$ and 22 ppm for $^{87}Sr/^{86}Sr$. Based on repeated runs of NBS981, the reproducibility of Pb isotope measurements is better than ±0.1%. Pb isotope ratios have been corrected relative to the average standard Pb isotopic compositions of Todt et al. (1993).

Results of Leaching

As mentioned above, isotope ratios were also measured on an unleached powder from Unit 990-13 to assess the efficacy of leaching. Epsilon Nd (t = 60 m.y.) shows a slight increase from 4.45 in the unleached to 4.88 in the leached sample. At the 2σ level, these values are statistically indistinguishable. There is, however, a marked reduction in $^{87}Sr/^{86}Sr$, from 0.70404 to 0.70349, perhaps resulting from the dissolution of zeolites and carbonate. We observed small increases in $^{206}Pb/^{204}Pb$ and $^{208}Pb/^{204}Pb$ after leaching, but $^{207}Pb/^{206}Pb$ shows no significant change. All of the changes in Pb isotopes are significantly less than the variations between samples.

Age Correction

Epsilon Nd is calculated for approximate time of eruption, where known (60 Ma for Southeast Greenland, Vøring Plateau, and Hatton Bank; present day for Iceland neovolcanic zone lavas). Sr and Pb isotope data are reported and plotted as present-day ratios, because we have no values for the Rb/Sr, U/Pb, and Th/Pb of the parental material (in this case, the leached residues).

Table 3. Values for international reference standards.

	BHVO-1	BIR-1	JB-1A
Major oxides (wt%, XRF by Copenhagen)			
SiO_2	50.02	47.82	
TiO_2	2.739	0.968	
Al_2O_3	13.65	15.49	
Fe_2O_3	11.92	11.27	
FeO	0.00	0.00	
MnO	0.17	0.17	
MgO	7.28	9.68	
CaO	11.42	13.31	
Na_2O	2.24	1.84	
K_2O	0.525	0.028	
P_2O_5	0.28	0.03	
Volatiles	–0.49	–0.6	
Total	99.752	100.003	
Trace elements (ppm, XRF by Edinburgh)			
Nb	19.8	0.6	
Zr	178.3	15.7	
Y	27.9	15.9	
Sr	403.9	108.3	
Rb	9.4	0.3	
Th	1.3	bdl	
Pb	2.5	3.1	
La	13.5	0.7	
Ce	39.6	3.1	
Nd	25.8	2.5	
Zn	104.0	69.4	
Cu	138.0	123.7	
Ni	121.9	165.4	
Co	288.8	382.2	
Cr	292.6	317.8	
V	133.6	9.0	
Ba	30.9	42.1	
Sc	21.7	16.3	
Ga	41.3	51.7	
Trace elements (ppm; INAA by Leicester)			
La			36.5
Ce			63.6
Nd			24.2
Sm			4.93
Eu			1.44
Gd			4.28
Tb			0.56
Yb			2.01
Lu			0.29
Ta			1.56
Th			8.98
Hf			3.55
Sc			28.8
Co			41.3
U			1.8

Note: XRF = X-ray fluorescence, bdl = below detectable levels, INAA = instrumental neutron activation analysis.

RESULTS

Site 988

Sample 988-1 is a light-REE-enriched tholeiite (Fig. 3). It has noticeably higher contents of total Fe, TiO_2, and most incompatible elements, especially Nb and Ta, than other analyzed samples from Leg 163 (Table 1). The shipboard scientific party observed that the low abundances of Ni and Cr are indicative of considerable fractionation, consistent with the three-phase phenocryst assemblage. The trace element abundance pattern of Unit 1 is similar to those of Tertiary basalts from Scoresby Sund and Site 407 in the Irminger Basin and a 52.5-m.y. sill recovered at Site 918 during Leg 152 (Figs. 1, 3). An interesting feature is the low K in all three samples in Figure 3.

Sample 988-1 has εNd (+5.3) and $^{87}Sr/^{86}Sr$ (0.7034) values that fall at the lower end of the field for Icelandic basalts (Fig. 4), an area of the plot that is dominated by Icelandic alkali basalts (Hémond et al., 1993). On the $^{207}Pb/^{204}Pb$-$^{206}Pb/^{204}Pb$ diagram, the sample plots between the fields for Atlantic MORB and Iceland (Fig. 5). Sample 988-1 has higher $^{208}Pb/^{204}Pb$ than MORB or Icelandic basalts, but is

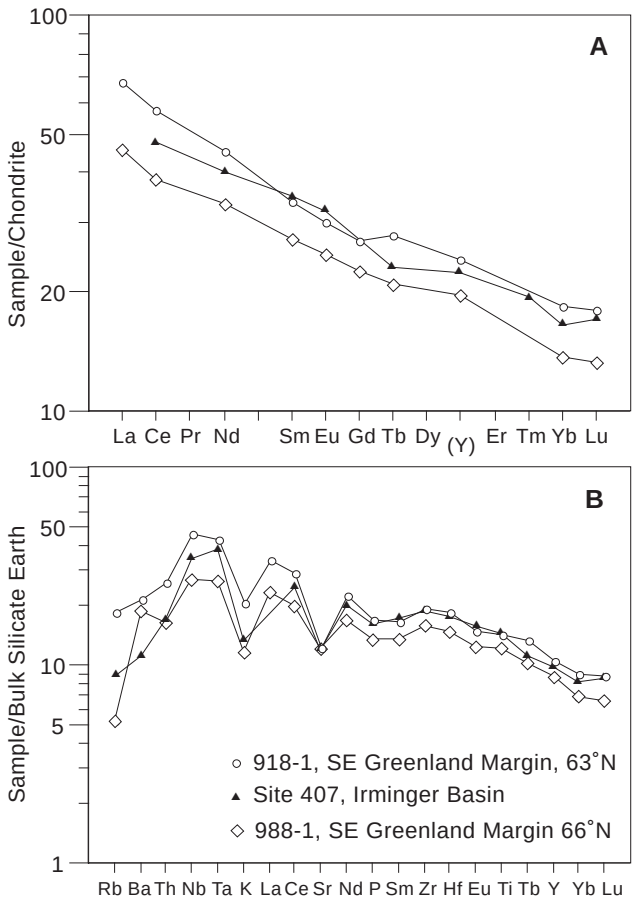

Figure 3. Chondrite-normalized **(A)** and bulk silicate Earth-normalized **(B)** patterns for basalts from Unit 988-1, Southeast Greenland margin; Unit 918-1, Southeast Greenland margin at 63°N (Fitton et al., 1998b); and Site 407 in the Irminger Basin (Sample 49/407/39-1, 55–59 cm; Luyendyk, Cann, et al., 1979). Chondrite-normalizing values from Nakamura (1974); bulk silicate Earth-normalizing values from McDonough and Sun (1995).

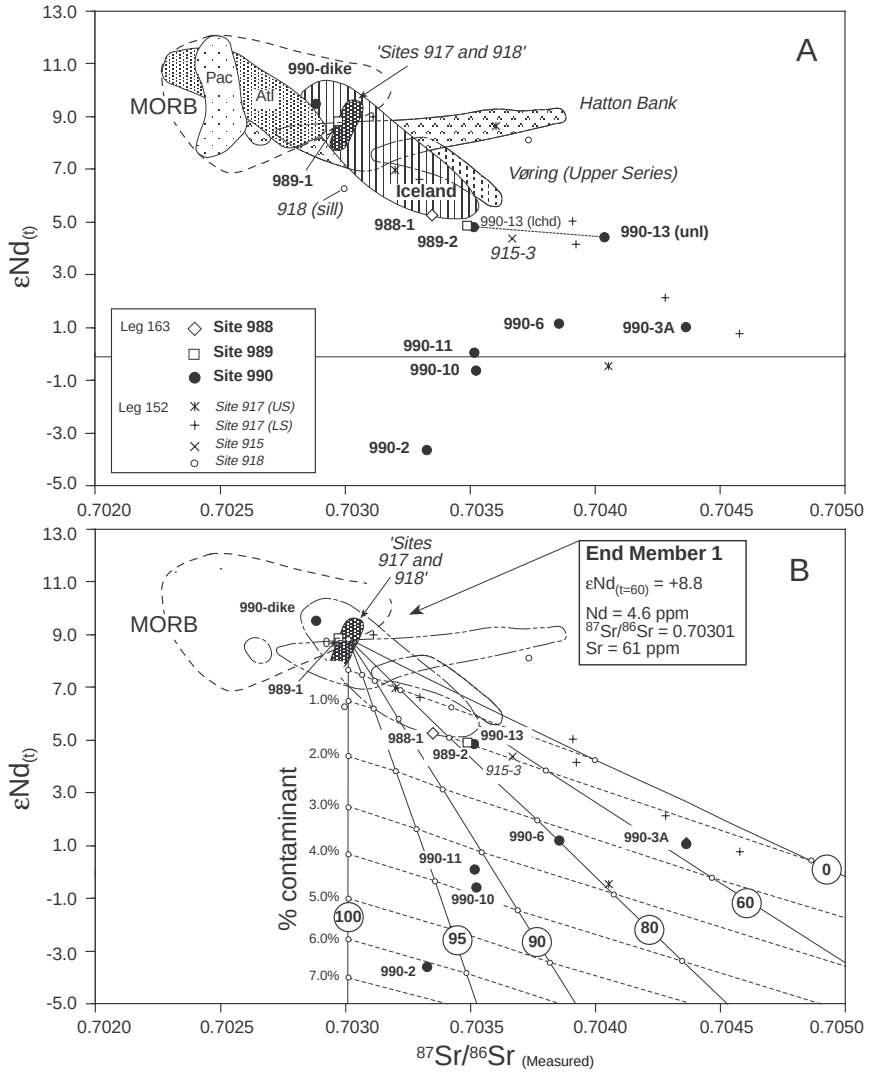

Figure 4. **A.** $\varepsilon Nd_{(t)}$ vs. $^{87}Sr/^{86}Sr_{(measured)}$ plot for basalts from the North Atlantic igneous province. Data sources for Leg 163 data are this paper; for Leg 152, Fitton et al. (1998a) (the field labeled "Sites 917 and 918" represents a cluster of data points for these two sites); mid-ocean-ridge basalts (MORB) (Pac = Pacific; Atl = Atlantic), Ito et al. (1987); Iceland, Sun and Jahn (1975), Cohen and O'Nions (1982), Elliott et al. (1991), Furman et al. (1991), and Hémond et al. (1993) and references therein; Hatton Bank, Macintyre and Hamilton (1984); Vøring Plateau (Site 642, Upper Series lavas only), Taylor and Morton (1989). Basalt from Unit 990-13 is plotted as leached (lchd) and unleached (unl) (see text for details). Note that many samples from the Lower and Middle Series of Site 917 are not shown because they fall well outside the boundary of this diagram (see Fig. 5). **B.** Same diagram as Figure 4A, but including three-component mixing lines between putative crustal and magmatic end-members. End-member 1 corresponds isotopically to the average, least-altered composition from Leg 152, Site 918 (Fitton et al., 1998a, 1998b) (εNd_{60} = 8.8; $^{87}Sr/^{86}Sr_{(measured)}$ = 0.70301; Sr [60.5 ppm] and Nd [4.55 ppm] abundances corrected for fractionation by addition of 30% olivine; see text). Two possible contaminants are considered—Archean granulite gneiss (εNd_{60} = –35; $^{87}Sr/^{86}Sr_{(measured)}$ = 0.7030; Nd = 25 ppm; Sr = 387 ppm) (Dickin, 1981) and Archean agmatite, Southeast Greenland (sample GSU324721 from Blichert-Toft et al., 1995) (εNd_{60} = –42; $^{87}Sr/^{86}Sr_{(measured)}$ = 0.7166; Nd = 89 ppm; Sr = 947 ppm) (see also Fig. 5). Six mixing lines are shown (by circled numbers), each with varying proportions of granulite and agmatite (100%, 95%, 90%, 80%, 60%, and 0% granulite); dashed lines indicate proportion of contaminant in basalt (0%, 0.5%, 1%, . . . 7%). Calculations assume simple bulk mixing and assimilation.

identical to basalts recovered from the SDRS at Site 918 during Leg 152 (Fig. 6); indeed, on both of the Pb isotope diagrams, the sample from Unit 988-1 generally falls within a subset of data that includes samples from both the Lower Series and Upper Series at Site 917, as well as from Site 918. Interestingly, none of the Leg 152 or 163 data show $^{206}Pb/^{204}Pb$ higher than 18.1, which is at the low end of the Iceland array, close to the field of Icelandic picrites and tholeiites from the Reykjanes Peninsula analyzed by Elliott et al. (1991). The $^{206}Pb/^{204}Pb$ values are also lower than those determined in Leg 49 tholeiites (Sites 407, 408, and 409) by Mattinson (1979).

Site 989

Although Unit 989-1 is texturally heterogeneous, comprising 69 subunits interpreted as pahoehoe lobes, shipboard analysis revealed little variation in the composition of the basalt. Seven samples were analyzed on board; MgO content ranged from 7.27% to 8.19%, Zr, from 41 to 56 ppm, and Ni, from 74 to 83 ppm. We have analyzed one sample from Unit 989-1. Although the basalt has a light-REE-depleted pattern (Fig. 7), La_n is slightly higher than Ce_n, resulting in a distinct concave-upward or "dish-shaped" light-REE distribution. (La_n refers to chondrite-normalized La.) The multielement plot (Fig. 7) shows relatively low abundances of the more incompatible elements. Very low abundances of K and Rb (also found in basalts from Sites 988, 918, and 407) may be caused by the effects of alkali leaching during weathering, although we cannot rule out the possibility that the low K and Rb is a primary feature; such low K and Rb abundances are also found in basalts from ocean islands such as St. Helena and, indeed, Iceland.

The basalt from Unit 989-1 has high εNd (~+9) and low $^{87}Sr/^{86}Sr$ (Fig. 4). Lead isotopes are similar to Unit 988-1 (Figs. 5, 6). In terms of all three isotope systems, Unit 989-1 overlaps with both the total MORB field and the field for Icelandic picrites.

The basalt from Unit 989-2 is slightly different from 989-1. The basalt is again light-REE depleted, with heavy-REE abundances identical with Unit 989-1. The light REEs, La through to Eu, do, however, have slightly higher abundances. Ba is noticeably enriched, and both K and Rb are not anomalously low. Abundances of some other incompatible elements are also higher in Unit 989-2. Unit 988-2 has significantly lower εNd and higher $^{87}Sr/^{86}Sr$ than 989-1, falling just below the Icelandic field in Figure 4, and it has a significantly lower $^{206}Pb/^{204}Pb$ ratio (<17) than Unit 989-1 (Figs. 5, 6).

An objective of drilling at Site 989 was to recover the oldest parts of the SDRS at 63°N. Seismic studies of the area (Larsen, Saunders, Clift, et al., 1994) suggested that the units drilled at Site 989 lie stratigraphically below, or overlap with, the succession at Site 917. However, shipboard and shore-based studies reveal marked differences between the lavas from the Lower Series at Site 917 and those from Site 989 (see Larsen et al., Chap. 7, this volume). None of the analyzed samples from the Lower Series at Site 917 have light-REE-

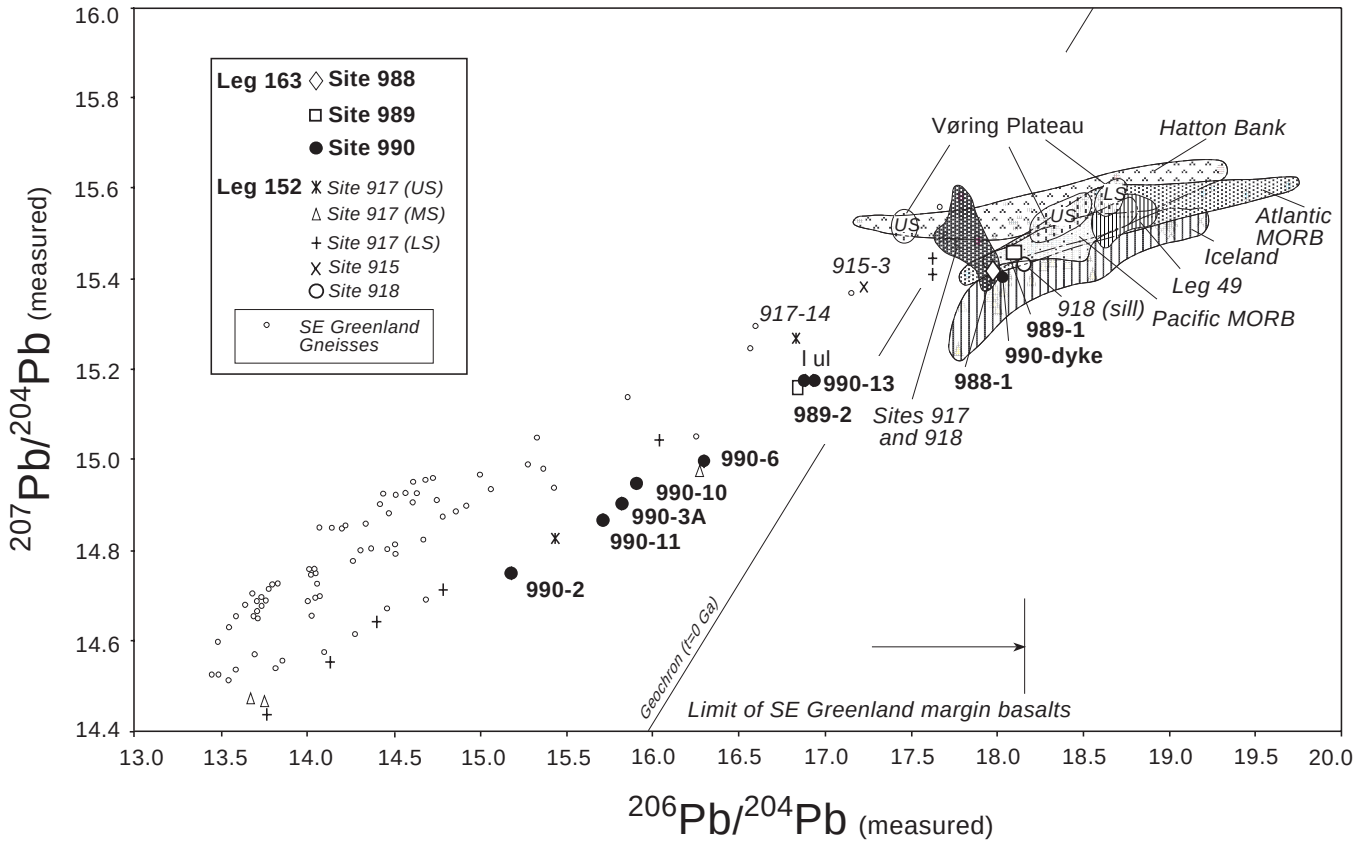

Figure 5. Basalts from the North Atlantic igneous province plotted on a $^{207}Pb/^{204}Pb$ vs. $^{206}Pb/^{204}Pb_{(measured)}$ diagram. Data sources for Leg 163 are this paper; Leg 152, Fitton et al. (1998a) (the field labeled "Sites 917 and 918" represents a cluster of data points for these sites); mid-ocean-ridge basalts (MORB), Ito et al. (1987); Iceland, Sun and Jahn (1975), Cohen and O'Nions (1982), Elliott et al. (1991), Furman et al. (1991), and Hémond et al. (1993) and references therein; Hatton Bank, Merriman et al. (1988); Vøring Plateau (Site 642, Upper and Lower Series lavas), Taylor and Morton (1989); Leg 49 (Sites 407–409, Irminger Basin), Mattinson (1979); Southeast Greenland gneisses (granulites, amphibolites and migmatites), Leeman et al. (1976), Taylor et al. (1992), and Kalsbeek et al. (1993).

depleted patterns like those from Site 989, and the contents of Ba and Sr are significantly higher than in the basalts from Site 989. The basalts from the Lower Series at Site 917 show a wide range of Pb, Nd, and Sr isotopes (Figs. 4, 5, 6, and 8), indicating that significant crustal contamination occurred in many of the magmas. Indeed, lavas from Site 989 more closely match lavas from the Upper Series from Site 917, which is dominated by basalts and picrites with light-REE-depleted and slightly light-REE-enriched patterns, the latter probably the result of crustal contamination (Fitton et al., 1998a, 1998b). In terms of Pb isotopes, Unit 917-14 is indistinguishable from 989-2, and several of the less contaminated samples from the Upper Series at 917 are similar to Unit 989-1 (e.g., Fig. 6). Unit 917-14 does, however, have much lower abundances of light REE, Nb, Ta, and heavy REE than does Unit 989-2.

Site 990

Six of the 13 lithologic units identified by the shipboard party, plus the basaltic dike found within Unit 990-12 (Tables 1, 2), have been analyzed in this study. The Site 990 samples show considerable diversity in incompatible element abundances and ratios, especially the large ion lithophile elements K, Rb, Ba, Th, and the light REE (Fig. 9). There is some downhole variation, with concentrations of incompatible elements decreasing with increasing depth (Larsen et al., Chap. 7, this volume). With the exception of the sample from Unit 990-2, which has a flat REE profile, all of the samples are light-REE depleted. Several of the samples have dish-shaped light- to middle-REE profiles, like Unit 989-1. The sample of the dike has a convex-upward "humpbacked" profile. The samples are divided into two broad groups in Figure 9, those with and those without dish-shaped REE profiles. The basalt from Site 915, Unit 3, is included for comparison.

On the multielement plots, Units 990-2, -3A, -6, -10, -11, and -13 show parallelism of the elements P through Lu, suggesting that the conditions of melting, and the composition of the source region, did not vary significantly throughout the eruption interval of these units. Unit 990-13 and the dike, however, have slightly but significantly lower relative abundances of heavy REEs and Sc, implying higher average pressures of melting (e.g., Fram et al., 1998). The elements Rb through Nd show much greater diversity. Ba/Ta ranges from 65 in the dike, to 1064 in Unit 990-11 (there is a general decrease in Ba/Ta and Ba/Zr downhole, with an anomaly at Unit 11). Downhole, Th/Hf also decreases from 0.26 in Unit 990-3A to 0.12 in Unit 990-13 (the dike has Th/Hf of 0.09).

The Site 990 samples show a wide range of isotope ratios. The dike has the highest εNd (+9.5) and lowest $^{87}Sr/^{86}Sr$ (0.7029) of any of the Legs 152 or 163 samples. It falls just within the Iceland field, and is well within the field of MORB, on the εNd-$^{87}Sr/^{86}Sr$ diagram (Fig. 4). Unit 990-13, from the bottom of the hole, has identical Nd, Sr, and Pb isotopes to Unit 2 of Hole 989B. Other samples from Hole

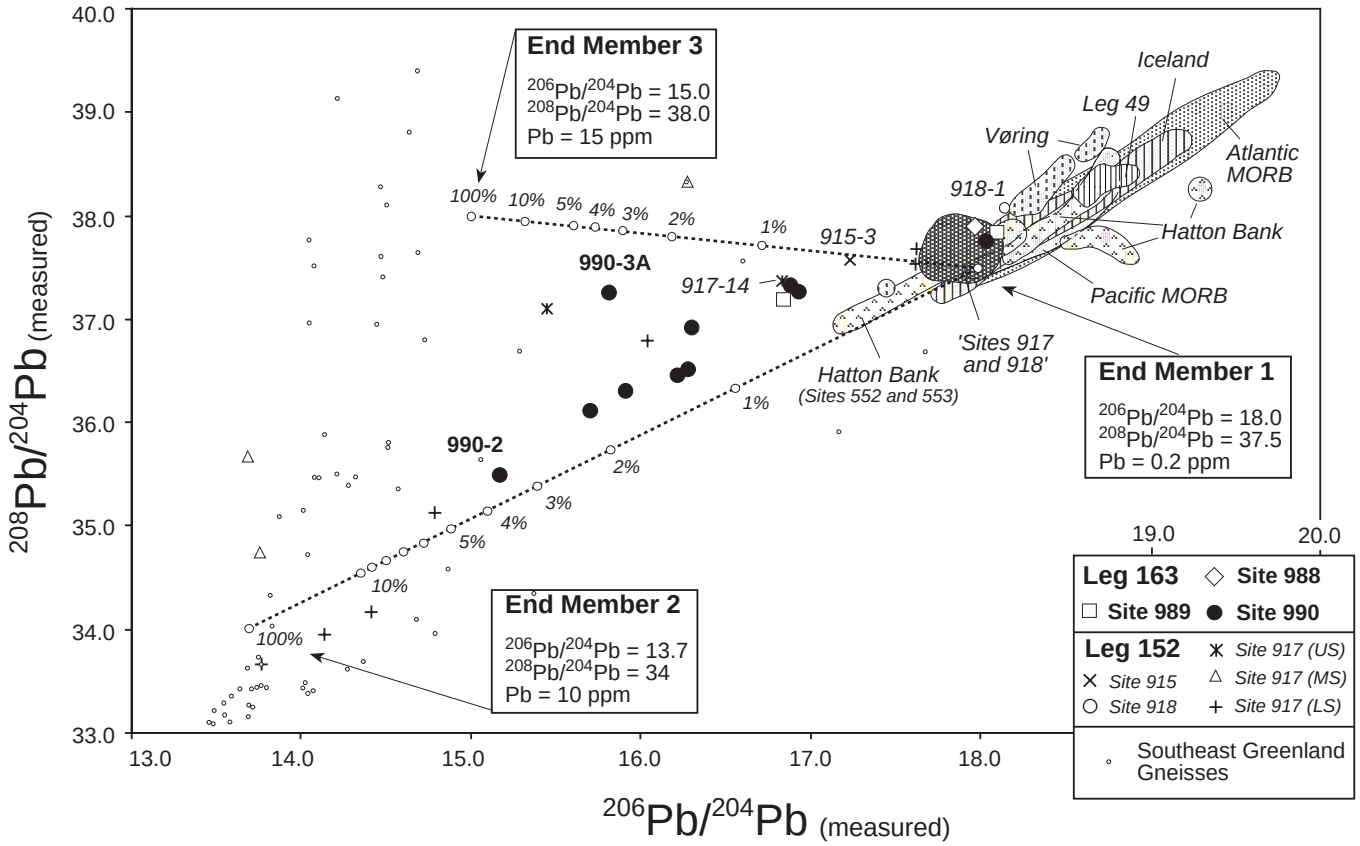

Figure 6. $^{208}Pb/^{204}Pb$ vs. $^{206}Pb/^{204}Pb_{(measured)}$ for basalts from the North Atlantic igneous province. Data sources are the same as for Figure 5. Two binary mixing lines are plotted for illustration purposes only and are not meant to be definitive. End-member 1 corresponds to average basaltic lava from Site 918 (data from Fitton et al., 1998a, 1998b), corrected for fractionation by addition of 30% olivine (Pb estimated assuming Ce/Pb = 25, after Hofmann et al., 1986 and Thirlwall et al., 1994). End-member 2 corresponds to granulite gneiss (e.g., Sheraton et al., 1973; Leeman et al., 1976; Dickin, 1981). End-member 3 corresponds to amphibolite gneiss (e.g., Dickin, 1981).

990A have significantly lower εNd, with Unit 990-2 having the lowest value of –3.7. Unit 990-3A has the highest $^{87}Sr/^{86}Sr$ (0.7044). The Pb isotope plots dramatically illustrate the range of compositions, with $^{206}Pb/^{204}Pb$ ranging from 18.03 (dike), which is close to the cluster of samples from Sites 918 and 988, down to 15.15 (Unit 990-2), which overlaps with the crustally contaminated samples from Site 917 (Figs. 5, 6). There are concomitant decreases in $^{207}Pb/^{204}Pb$ and $^{208}Pb/^{204}Pb$, although Unit 990-3A, which has the highest $^{87}Sr/^{86}Sr$, also has high $^{208}Pb/^{204}Pb$. Unit 915-3 is encompassed by the chemical and isotopic range of samples from Site 990, indicating coeval eruption; this is not surprising given the close proximity of the two sites.

DISCUSSION

The Role of Crustal Contamination

Despite taking samples from the least altered parts of the cores, it is apparent that most, if not all, of the samples have undergone alteration with conversion of mesostasis and olivine to smectite clays. Some portions of the core, especially those close to veins, show development of zeolites in vesicles, and mobilization of Cu is especially evident in the core from Hole 990A (Duncan, Larsen, Allan, et al., 1996). It is, therefore, likely that abundances of some trace elements will have been affected by secondary processes during weathering in a subaerial or subaqueous environment and/or during subsequent (slight) hydrothermal activity. The details of the alteration process will be presented elsewhere in this volume (Teagle and Alt, Chap. 13, this volume).

The effects of secondary processes on isotope ratios are illustrated by the leaching experiment undertaken on the sample from Unit 990-13. Whereas both εNd and Pb isotope ratios show insignificant change, $^{87}Sr/^{86}Sr$ is reduced from 0.7040 to 0.7035. This suggests that the measured isotope ratios in other, leached, samples reflect magmatic values, albeit ones uncorrected for the effect of ageing in the case of Sr and Pb isotope ratios. Elements considered as mobile in a variety of weathering and alteration conditions (e.g., Rb, K, and, possibly, Ba and Sr) are interpreted with caution, although we note the consistent relationship of, for example, Ba/Ta with $^{206}Pb/^{204}Pb$ (Fig. 10), suggesting that the broad changes in relative Ba abundance are not caused by secondary processes. The other elements used here (Th, REEs, Zr, Hf, Nb, Ta, Sc, Ti, and P) are considered as immobile in basaltic rocks that have undergone the extent of alteration observed in the Leg 163 (and Leg 152) cores.

The variation in element ratios (such as La/Yb, Ba/Zr, Ba/Ta, Nb/Zr, and Th/Ta) and in isotope ratios cannot be explained solely by fractional crystallization or melting of mantle peridotite. Varying amounts of assimilation of a lithospheric component with high concentrations of light REEs, Ba, and variably radiogenic Sr but unradiogenic Pb are required. Fitton et al. (1998a) have argued that the contaminants of Lower and Middle Series lavas from Site 917 were ancient amphibolites and granulites. Both rock types outcrop along the adjacent Greenland coast. Analyses of similar rocks from Scotland

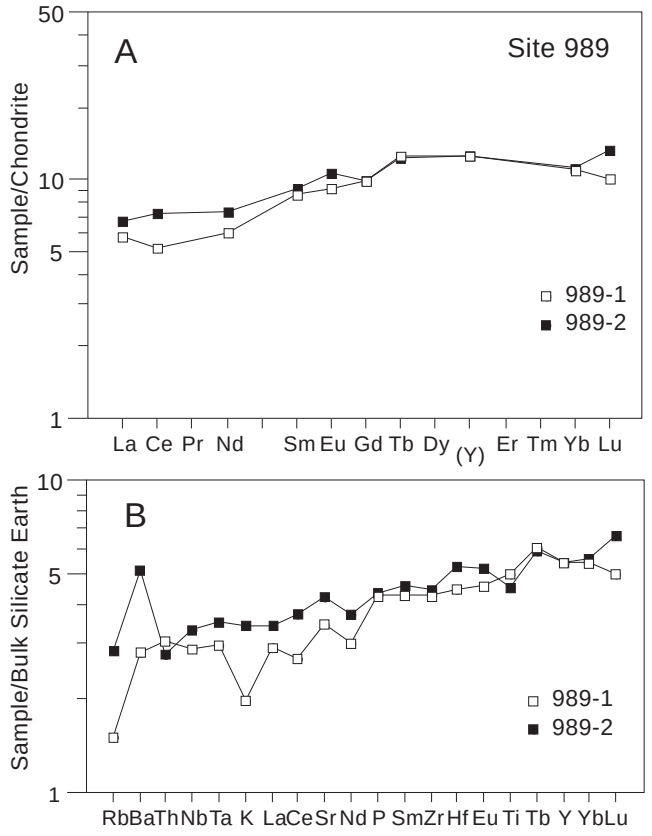

Figure 7. Chondrite-normalized **(A)** and bulk silicate Earth-normalized **(B)** patterns for basalts from Units 989-1 and 989-2, Southeast Greenland margin. Chondrite-normalizing values from Nakamura (1974); bulk silicate Earth-normalizing values from McDonough and Sun (1995).

(Dickin, 1981) and Greenland (Leeman et al., 1976; Taylor et al., 1992; Kalsbeek et al., 1993) demonstrate at least semiquantitatively that contamination can produce the wide spectrum of Pb-, Nd-, and Sr-isotope ratios observed in the Site 917 lavas (e.g., Figures 4, 5, 6, and 8). The low εNd, $^{87}Sr/^{86}Sr$, and $^{20x}Pb/^{204}Pb$ of many of the Lower Series lavas appears to be the result of assimilation of ancient granulite with long-term low Sm/Nd, Rb/Sr, Th/Pb, and U/Pb. The Middle Series lavas, however, have significantly higher $^{87}Sr/^{86}Sr$ and $^{208}Pb/^{204}Pb$, implying that the contaminant had higher time-integrated Rb/Sr and Th/Pb ratios, perhaps Archean or Proterozoic amphibolite. This has led to the intriguing suggestion that the magmas were contaminated at progressively shallower depths, the Lower Series by deep, lower crustal granulites, and the Middle Series by shallower, perhaps middle or upper crustal amphibolites (Fitton et al., 1998a). Few of the succeeding Upper Series lavas from Site 917 show signs of extensive contamination (and neither does the analyzed basalt sample from Site 915), but the high $^{208}Pb/^{204}Pb$ and $^{87}Sr/^{86}Sr$ of those that are contaminated (e.g., Figs. 4, 6) imply that contamination continued to be dominated by amphibolitic rather than by granulitic material.

We have included modeled mixing curves on Figures 4, 6, and 9. These curves merely illustrate possible mixing arrays using end-members that may correspond to real rocks along the Southeast Greenland margin. However, it is important to stress at the outset that the models are not unique; they merely indicate a range of types and amounts of potential contaminants. We begin our discussion with Pb isotope ratios, which are most sensitive to the effects of crustal contamination. The composition of the (uncontaminated) basaltic end-member (End-member 1 on Figs. 5, 6, and 10) may be estimated from the Legs 163 and 152 data, especially the data from Site 918.

Site 918 is located on the main outcrop of SDRS, some 50 km to the southeast of the continent-ocean transition. Although it is not possible to completely rule out the presence of a fragment of continental crust underneath this site, this is thought to be highly unlikely. Several samples from the Upper Series at Site 917, from Units 988-1 and 989-1, and the dike from Site 990 all plot within or close to the field of Site 918 and the Icelandic basalts in Pb isotope space (Figs. 5, 6). These data suggest that the uncontaminated, sublithospheric mantle beneath this margin had a $^{206}Pb/^{204}Pb$ of ~18 and $^{208}Pb/^{204}Pb$ of ~37.5, and we use these values for the composition of the parental magma. Estimating the abundance of Pb is more difficult, although the mixing models are very sensitive to this parameter. We have assumed that the average Pb content of Site 918 lavas is 0.3 ppm, based on a Ce/Pb ratio of 25 (Hofmann et al., 1986) and an average Ce abundance of 7.5 ppm (Fitton et al., 1998b). The primary magma at Site 918 would have had significantly less Pb than this, because the analyzed lavas have clearly undergone significant fractionation of olivine (they are not primary melts) (e.g., L.M. Larsen et al., 1998). We have back calculated the Pb content by adding 30% olivine to the melt, achieving a Pb concentration of ~0.2 ppm (assuming that $Kd_{Pb}^{olivine} = 0.0$).

It could be argued that the Pb content of the primary magmas at Sites 989 and 990 was higher than 0.2 ppm because the average depth of melting was greater than at Site 918. That the Sites 989 and 990 magmas were erupted through continental lithosphere implies the presence of a lithospheric lid, which may have shortened the melt column (cf., Fram et al., 1998). This would have resulted in increased concentrations of incompatible elements in the pooled primary melts. However, we note that the Sc (and heavy REE) abundances of the lavas from Sites 989 and 990 are not significantly different from those in lavas from Site 918. Indeed, Zr/Sc ratios are actually lower in some of the Sites 989 and 990 basalts relative to those from Site 918 (e.g., Zr/Sc in Units 989-1 and 990-13 is 0.8 and averages 0.97 at Site 918). For comparison, Zr/Sc in prebreakup lavas from Site 917 exceed 1.0. This suggests that the influence of a continental lithospheric lid on the melting process may have been similar for the lavas erupted at Sites 915, 918, 989, and 990; in other words, by the time of the eruption of the Sites 915, 989, and 990 basalts, the magmatism was at a fully fledged rift zone (a more detailed discussion is presented in Larsen et al., Chap. 7, this volume). Note that the Ce abundance in Units 989-1 ($^{206}Pb/^{204}Pb = 18.1$, at the high end of the Pb isotope array) is 4.5 ppm, indicating a Pb content of 0.18 ppm. The sample from the dike has a significantly higher Ce abundance (10.7 ppm) and, by inference, Pb (0.43 ppm), but it also has higher Zr/Sc, implying smaller degrees of partial melting of the source. Despite these uncertainties, we believe that the Pb concentration in the primary melt for most units from Sites 915, 918, 989, and 990 is unlikely to have exceeded 0.2 ppm, but may have been slightly higher (0.3–0.4 ppm?) in the magma that supplied the dike.

Two possible crustal end-members are included in Figure 6. End-member 3 has $^{206}Pb/^{204}Pb = 15$, $^{208}Pb/^{204}Pb = 38$, and Pb = 15 ppm. These values are similar to those for Archean amphibolite-grade gneisses from Scotland (Dickin, 1981), reflecting a high time-integrated Th/U ratio. End-member 2 has much lower $^{206}Pb/^{204}Pb$ (13.7) and $^{208}Pb/^{204}Pb$ (34), more closely resembling an Archean granulite. The value of 13.7 for $^{206}Pb/^{204}Pb$ was estimated from Figure 9. Samples from Sites 989 (Unit 2) and 990 plot between these two extremes, implying that the contaminant has a hybrid composition. In either case, the amount of contaminant does not exceed 5%, assuming bulk assimilation. Note that neither model satisfactorily accounts for the isotopic signature of the basalts from the Lower Series at Site 917 (Fig. 5), because very large amounts of contamination are required (almost 100%), which is untenable. Either decreasing the amount of Pb in the primary melt, increasing the amount of Pb in the contaminant, decreasing the $^{206}Pb/^{204}Pb$ ratio of the contaminant, selectively

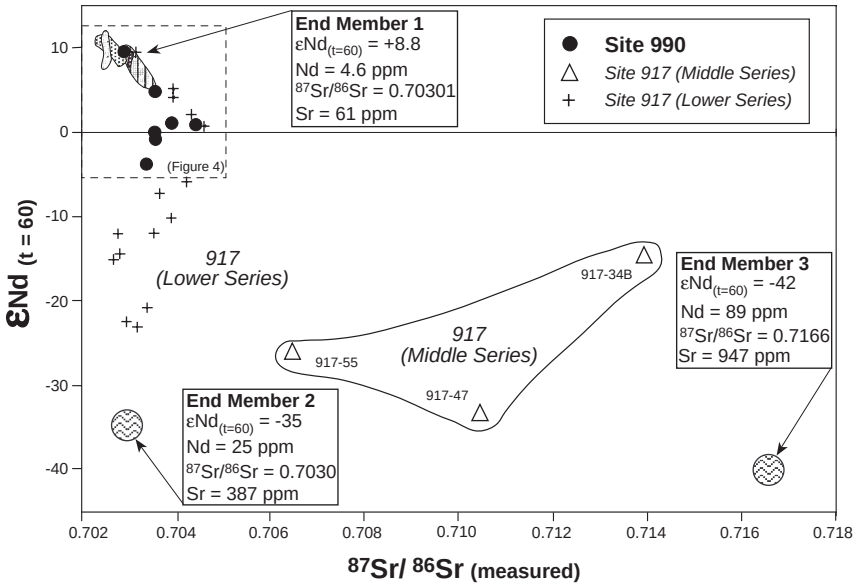

Figure 8. εNd vs. $^{87}Sr/^{86}Sr_{(measured)}$ for basalts from Legs 152 and 163, showing the full range of isotope values in the Middle and Lower Series from Site 917, and the compositions of the main end-members used in modeling (see Fig. 4 and text). Data sources are Fitton et al. (1998a) for Site 917 and sources in Figure 4 caption. Dashed lines indicate the extent of Figure 4.

melting Pb-rich fractions from the rock, or a combination of these is necessary to account for these extremely low $^{206}Pb/^{204}Pb$ values.

Similar amounts of contamination are indicated by modeling the εNd and $^{87}Sr/^{86}Sr$ data (Figs. 4, 8). We estimate that End-member 1, the primary basalt magma, has Nd and Sr contents of 4.55 and 60.5 ppm, respectively, and εNd = +8.8, and $^{87}Sr/^{86}Sr$ = 0.7030. Two possible contaminants are used in this model, an Archean granulite gneiss (εNd_{60} = –35; $^{87}Sr/^{86}Sr_{(pd)}$ = 0.7030; Nd = 25 ppm; Sr = 387 ppm; Dickin, 1981) and a high Rb/Sr Archean agmatitic granulite from Southeast Greenland (sample GGU324721 from Blichert-Toft et al., 1995: εNd_{60} = –42; $^{87}Sr/^{86}Sr_{(pd)}$ = 0.7166; Nd = 89 ppm; Sr = 947 ppm). The latter is similar to Dickin's (1981) Scottish amphibolite gneiss in terms of Nd and Sr isotope ratios (unfortunately, there are no Pb isotope data available for this sample). Several combination mixing lines are also shown on Figure 4, with 95%, 90%, 80%, and 60% granulite end-member, respectively. Note that Unit 990-2, which has the lowest εNd_{60} and low $^{87}Sr/^{86}Sr$, also has the lowest $^{206}Pb/^{204}Pb$, consistent with assimilation of Archean granulite.

The effect on trace element concentrations of addition of putative crustal material to an estimated primary magma is shown in Figures 10 and 11. In Figure 10, the crustal contaminant is assumed to be similar to Archean granulite, with $^{206}Pb/^{204}Pb$ = 13.7, Ba = 1000 ppm, Pb = 10 ppm, and Ta = 0.3 ppm. A contaminant with higher Ba/Ta and Pb (for example, sample GGU324721 from Blichert-Toft et al., 1995) would give an even better fit to the observed data but would not, alone, satisfy the Sr isotope data. Multielement plots are shown in Figure 11. Addition of 0.5 to 2 wt% of sample GGU324721 to the Site 918 primary magma is sufficient to replicate the patterns in the most contaminated lavas, although the agreement for K, Rb, and Sr is poor. Addition of a hybrid contaminant, involving a low-Rb granulite gneiss, would allow addition of slightly more contaminant and may more accurately replicate the low Rb/Ba ratios in Units 990-2, 990-3, and 990-11 (see Fig. 9). Similarly, the dish-shaped profile of the light REE could be more accurately produced if the contaminant had a slightly higher La/Ce ratio. The variation in major elements is broadly consistent with these amounts of contamination. For example, the basalts with the highest SiO_2 (i.e., from Units 990-2 and 990-11) have the lowest $^{206}Pb/^{204}Pb$ of the Leg 163 samples.

Basalts from Hatton Bank on the southwest corner of the Rockall Plateau (Fig. 1) show a different pattern of contamination to those from Southeast Greenland. These basalts are strongly light-REE depleted and, with low abundances of Nb and Ta, similar to normal MORB (e.g., Joron et al., 1984; Fitton et al., 1997; Brodie and Fitton, 1998), so the amount of contamination is necessarily small. However, Pb isotope studies show that some samples, especially those from Sites 552 and 553, have been contaminated by material with low $^{206}Pb/^{204}Pb$ but high $^{207}Pb/^{204}Pb$ (Morton and Taylor, 1987) (Fig. 5), possibly Proterozoic Laxfordian or Grenvillian granulites similar to those recovered from the Rockall Plateau (Miller et al., 1973).

Lavas from Site 642 on the Vøring Plateau show yet a third pattern of contamination, different from those recorded in lavas from Southeast Greenland and Hatton Bank. The thick succession of lavas drilled during Leg 104 was divided into an upper series of 120 flow units of basalt and a lower series comprising peraluminous, light-REE-enriched dacite (13 flows), some of which contain cordierite crystals, and 5 flows of andesite (Eldholm, Thiede, Taylor et al., 1987; Viereck et al., 1988, 1989). The upper series basalts plot within or close to the fields of MORB and Iceland on Pb isotope plots (with one sample having low $^{206}Pb/^{204}Pb$). On the εNd-$^{87}Sr/^{86}Sr$ diagram, they overlap with Iceland with slight displacement to higher $^{87}Sr/^{86}Sr$. These data indicate that the amount of crustal contamination of the upper series lavas is slight. The lower series lavas, on the other hand, have high $^{87}Sr/^{86}Sr$ (>0.709) and moderately low εNd (~–5) (Taylor and Morton, 1989). However, they have higher $^{206}Pb/^{204}Pb$ than the upper series basalts (Fig. 5). This is the opposite of what is observed in Southeast Greenland and Hatton Bank and implies that the crustal component in the Vøring Plateau samples is dominated by a long-term, high U/Pb and Rb/Sr component. Similar contamination is observed in some Faeroes lavas (e.g., Sample K1; see Gariépy et al., 1983).

Composition of Sublithospheric Melts

An important goal of both Legs 152 and 163 was to assess the contribution of the ancestral Iceland plume to the magmatism along the Southeast Greenland margin. Several end-member models have been proposed to explain the formation of volcanic rifted margins and related large igneous provinces, such as continental flood basalts and oceanic plateaus.

1. Magmatism is a function of the arrival of a large, hot plume head that impacts at the base of the lithosphere, decompresses,

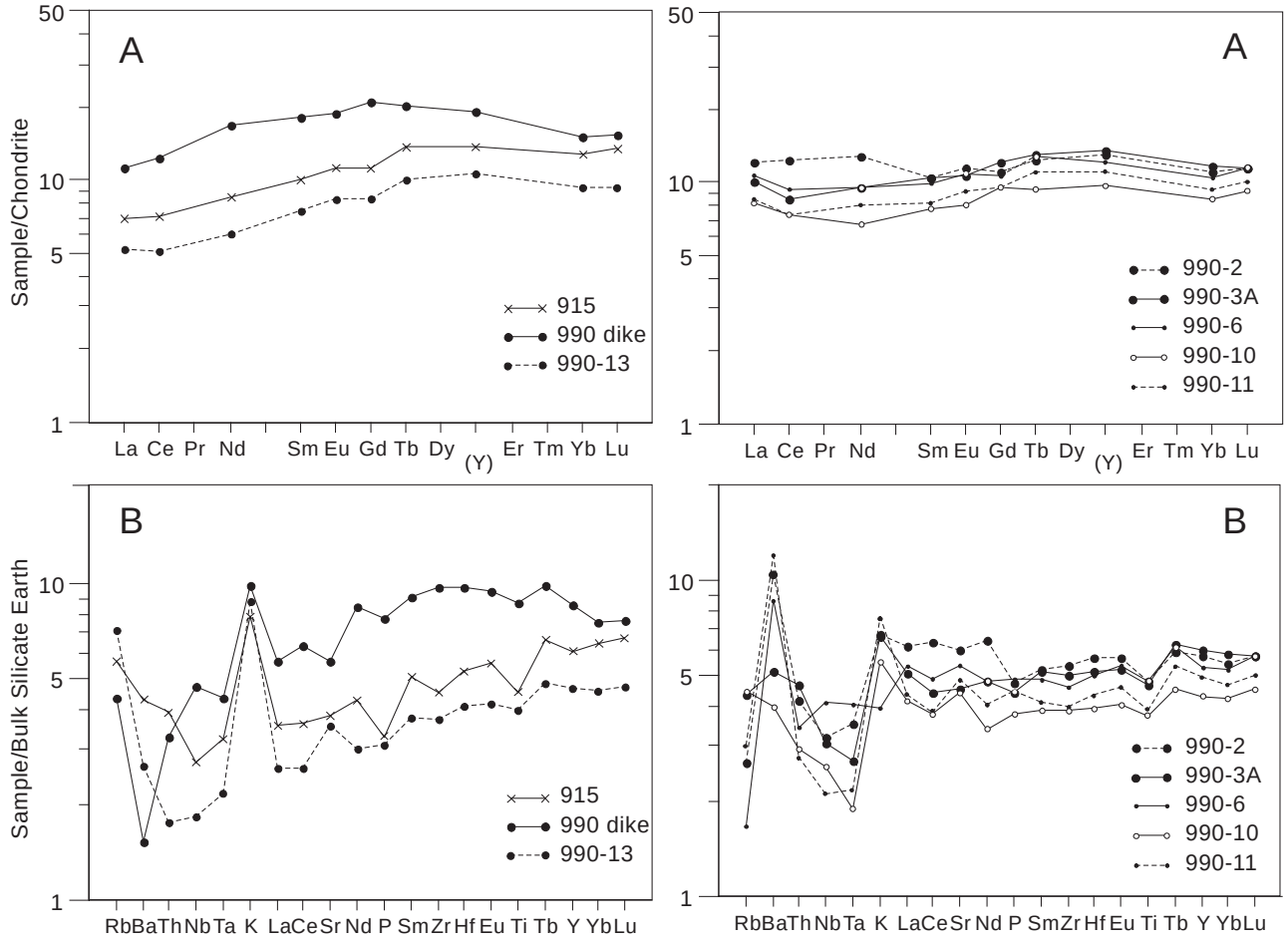

Figure 9. Chondrite-normalized **(A)** and bulk silicate Earth-normalized **(B)** patterns for basalts from Sites 915 and 990, Southeast Greenland margin. Chondrite-normalizing values from Nakamura (1974); bulk silicate Earth- normalizing values from McDonough and Sun (1995).

and melts (Richards et al., 1989; Campbell and Griffiths, 1990). Impact and uplift of the lithosphere may assist with continental fragmentation.

2. The lithosphere rifts and separates above a large-diameter plume head, which decompresses and produces large volumes of basaltic magma (White and McKenzie, 1989).
3. The lithosphere separates above asthenospheric mantle that is at, or close to, ambient temperature, and excess magmatism is generated by enhanced convection (Mutter et al., 1988).

The composition of the basalts erupted along the volcanic rifted margin may distinguish models 1 and 2 from 3 if the composition of the plume mantle is distinct from that of ambient MORB mantle and if the effects of crustal contamination have not masked the sublithospheric signature. An accurate knowledge of the timing of rifting and magmatism is required to distinguish between models 1 and 2.

Basalts from the neovolcanic zone on Iceland show considerable isotopic and trace element diversity, which shows that the underlying mantle is chemically heterogeneous (Wood et al., 1979; Hémond et al., 1993; Kerr et al., 1995) (Figs. 4–6). Although some workers have proposed that the variation in Icelandic basalts is a result of mixing between a MORB-mantle component and an enriched-mantle component (e.g., Hart et al., 1973; Schilling, 1973), this cannot explain the reduced $^{207}Pb/^{204}Pb$ in Icelandic basalts relative to MORB (Thirlwall et al., 1994; Thirlwall, 1995). Rather, the sub-Icelandic mantle comprises both depleted and less-depleted components that are intrinsic to the plume (e.g., Kerr et al., 1995; Saunders et al., 1997).

Thus, any attempt to "fingerprint" the composition of the Tertiary sublithospheric mantle underlying Greenland and northwest Europe needs to take into account the isotopic and elemental heterogeneity of the present-day Iceland plume. It is likely that the putative Tertiary plume would have been similarly heterogeneous. There is a further complication in that ambient MORB mantle, surrounding the chemical plume, also contributes to the Tertiary magmatism and, indeed, to present-day magmatism along the mid-Atlantic Ridge (Taylor et al., 1997; Saunders et al., 1997; Fitton et al., 1997, 1998b).

Bearing in mind that the majority of the samples recovered from Leg 163 are contaminated by lithosphere, can we be sure that any are uncontaminated, and, thus, allow us to fingerprint the sublithospheric mantle? In the previous section, we have argued that basalts from Site 918, and some basalts from Sites 917, 989, and 990, are uncontaminated, implying that the sublithospheric mantle beneath this margin had a $^{206}Pb/^{204}Pb$ = ~18, εNd = +8.8, and $^{87}Sr/^{86}Sr$ = ~0.7030. It was also light-REE depleted, resembling both normal MORB and light-REE-depleted Icelandic basalts. Indeed, these isotopic characteristics are found in some Icelandic basalts and picrites and some Atlantic MORB (mostly from ridge segments close to plumes). The bulk of the Pacific and Atlantic MORB have lower $^{87}Sr/^{86}Sr$ than the Southeast Greenland margin and Icelandic lavas (e.g., Cohen et al., 1980; Cohen and O'Nions, 1982; Ito et al., 1987). Note, however, that most

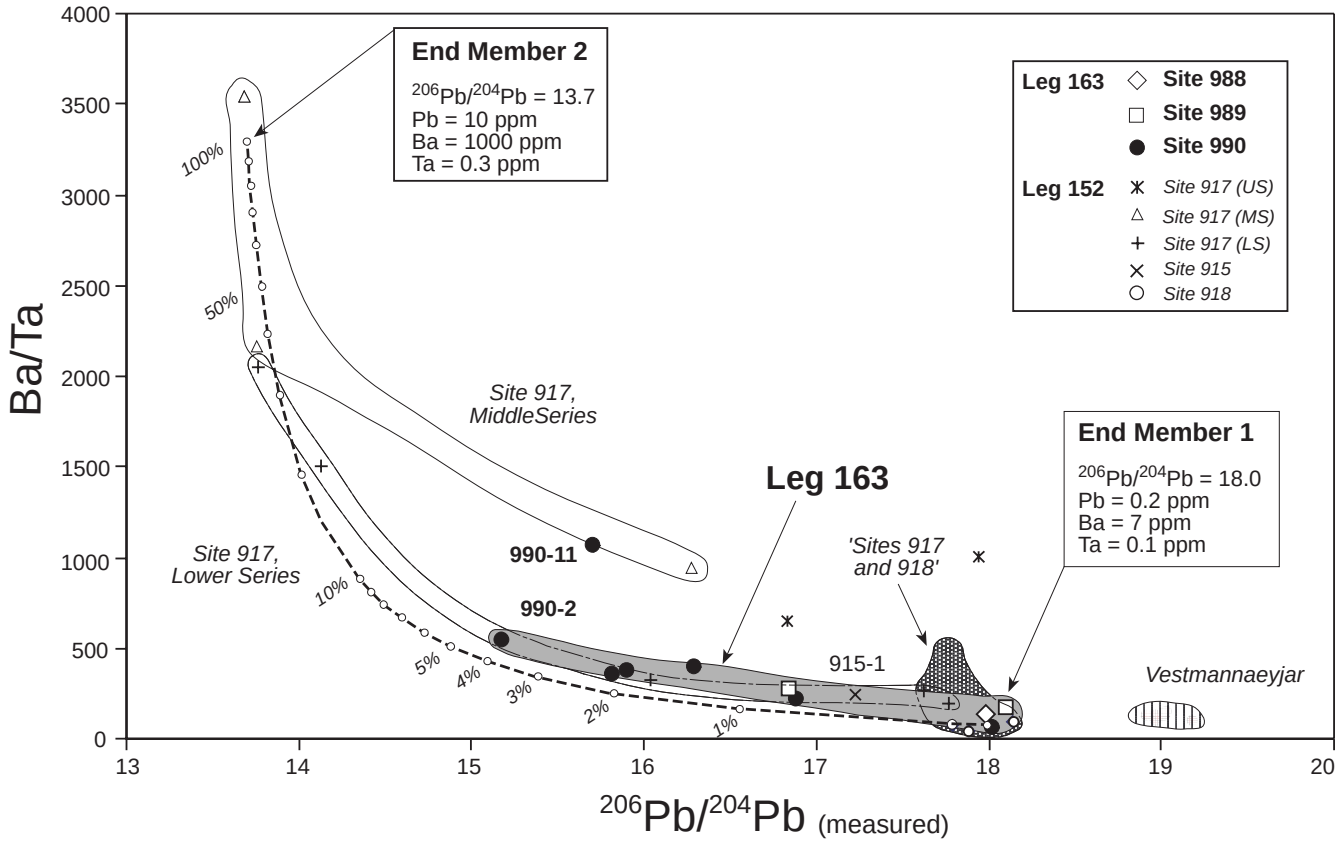

Figure 10. Ba/Ta vs. $^{206}Pb/^{204}Pb_{(measured)}$ for basalts from Leg 163 (this paper), Iceland (Furman et al., 1991), and lavas from Leg 152 (Fitton et al., 1998a, 1998b). Field labeled "Sites 917 and 918" includes a cluster of apparently uncontaminated basalts recovered during Leg 152. Mixing line shows simple binary mixing between End-member 1, average basaltic lava from Site 918 lava (data from Fitton et al., 1997, 1998b) (Pb abundance estimated assuming Ce/Pb = 25, after Hofmann et al., 1986 and Thirlwall et al., 1994) corrected for fractionation by adding 30% olivine; and End-member 2, Archean gneiss (composite sample using data from Sheraton et al., 1973 and others, see text; Ta = Nb/16.5; $^{206}Pb/^{204}Pb$ from observed distribution of Leg 152 data).

of the Southeast Greenland lavas have slightly higher $^{207}Pb/^{204}Pb$ than does Iceland.

Many lavas from the Vøring Plateau and Hatton Bank have higher $^{206}Pb/^{204}Pb$ than those from Southeast Greenland, but it is not possible to completely eliminate contamination by crustal material with a high $^{206}Pb/^{204}Pb$ as a factor in even the Vøring upper series lavas. The lavas recovered from the Irminger Basin during Leg 49 have $^{206}Pb/^{204}Pb$ greater than 18.5, straddling the MORB-Iceland fields. The Leg 49 sites lie on a mantle flow line between Site 988 and the Reykjanes Ridge, so it is not surprising that they have an Icelandic signature, although it is surprising that the Site 988 basalts do not also have higher $^{206}Pb/^{204}Pb$.

With the possible exception of εNd and $^{87}Sr/^{86}Sr$ values, which suggest Icelandic affinities, the isotope data do not provide an unequivocal discrimination between MORB and Icelandic sources for the Southeast Greenland magmas. The uncontaminated precursors for the Sites 989, 990, and 915 (and the Upper Series from Site 917) basalts were probably all light-REE depleted, resembling normal MORB. Rare earth elements are of little use as discriminants, however, because light-REE-depleted basalts are erupted in Iceland as well as along mid-ocean ridges. Discrimination by other methods must be sought. Fitton et al. (1997, 1998b) have shown that Icelandic basalts have interelement ratios involving Zr, Y, and Nb that are distinct from those found in normal MORB. This is a reflection of the relatively higher abundances of Nb in Icelandic (and other ocean island) basalts and, by implication, their mantle source. The relationship holds even for Icelandic basalts that are strongly light-REE-depleted and which, in several other ways, closely resemble normal MORB (Fig. 12). Fitton et al. (1997) argue that the Nb/Y vs. Zr/Y diagram is insensitive to low-pressure fractionational crystallization and that the differences between MORB and Icelandic basalts reflect real difference in their mantle sources.

Light-REE-depleted basalts from Site 918 plot in the array defined by Icelandic basalts on the Zr/Y-Nb/Y diagram, whereas similarly depleted basalts from Hatton Bank plot below the array, in the MORB field (Fig. 12) (Fitton et al., 1997, 1998b). All of the Leg 163 basalts fall in, or very close to, the Icelandic array. The clear exception is the dike from Site 990, which is clearly MORB-like, a fact that corroborates the high εNd and low $^{87}Sr/^{86}Sr$ values for this sample (Fig. 4). Note that two of the samples from Site 990, which fall just within the MORB field (from Units 990-2 and -11), are also the most contaminated samples we analyzed, although most crustal contaminants lie far to the right (high Zr/Y) on the diagram.

The ΔNb function can be used to express the excess or deficiency in Nb relative to the lower bound of the Iceland array (Fig. 13) (Fitton et al., 1997). Positive values of ΔNb imply that the basalts were derived from an Icelandic source, whereas negative ΔNb implies derivation from depleted, normal MORB, upper mantle. Figure 13 plots ΔNb for all of the analyzed basalts from the 63°N transect (Sites 915, 917, 918, 989, and 990) in their stratigraphic positions. Note that the depths are relative and not absolute and that we have omitted gaps between successions. As pointed out by Fitton et al. (1998b), the Site 917 basalts are derived mainly from a MORB source (with the occasional input from a high ΔNb Icelandic source). The source switches

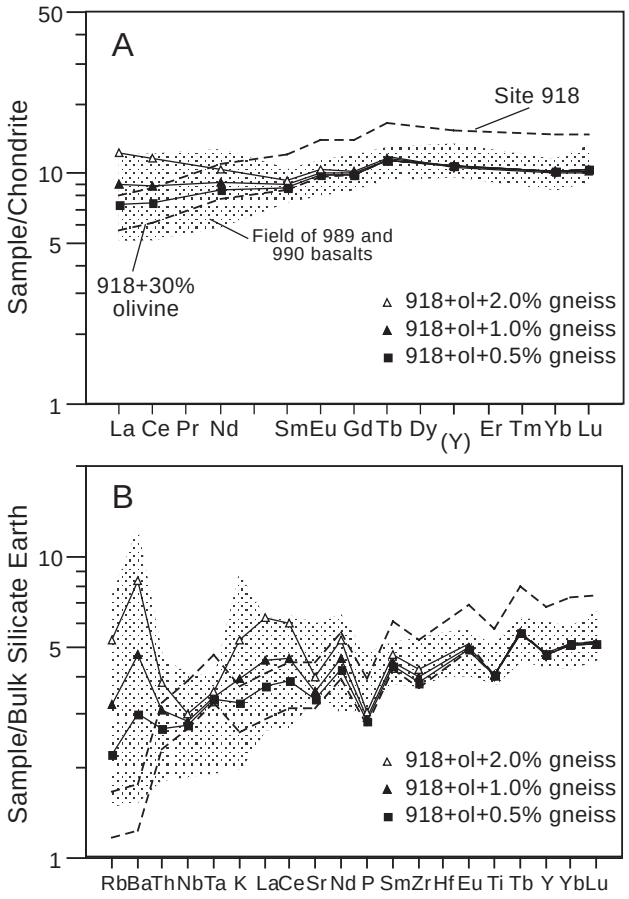

Figure 11. Chondrite-normalized **(A)** and bulk silicate Earth-normalized **(B)** patterns for modeled basalt compositions. The upper dashed lines in both diagrams are average compositions for the lavas from Site 918. The lower dashed lines in each diagram represent the putative parental magma to Sites 989 and 990, produced by addition of 30% olivine to the Site 918 composition. The lines represented by the square, filled triangle, and open triangle represent addition of 0.5%, 1.0%, and 2.0%, respectively, of gneiss GGU324721 to this magnesian parental melt. The shaded zones show the fields for basalts from Sites 989 and 990 (omitting the dike from Site 990). The model replicates reasonably well the measured data, except for Sr and some units (e.g., 990-13, 990-10) that have very low abundances of the more incompatible elements. Data sources for Site 918 basalts are average of Units 918-8B, -12B, -13B, and -15 from Fitton et al (1998b); gneiss GGU324721, Blichert-Toft et al. (1995). Chondrite-normalizing values from Nakamura (1974); bulk silicate Earth-normalizing values from McDonough and Sun (1995).

dramatically to Icelandic between the Site 917 and Site 915 lavas, with the occasional excursion to negative ΔNb (especially in the dike from Site 990).

The implication of these data is that the mantle source that fed the lavas at Sites 915, 918, 989, and 990 was light-REE depleted, but with a predominantly Icelandic signature. The frequent involvement of Icelandic mantle in the formation of the SDRS along the Southeast Greenland margin suggests that the Iceland plume was supplying material as far south as 63°N during the Paleocene-Eocene, corroborating the observation of voluminous magmatism along this volcanic rifted margin. Magmas erupted on Hatton Bank, farther from the ancestral plume axis, are also light-REE depleted, but also have MORB-like Zr/Y-Nb/Y, suggesting that the chemical influence of the Iceland plume had not reached that far south, although the thermal signature had.

The data presented in this paper, therefore, support the idea that the ancestral Icelandic plume contributed to the formation of the SDRS along the Southeast Greenland margin at both 63°N and 66°N. This supports previous models (e.g., White and McKenzie, 1989) that SDRS formation is linked to the extension and decompression melting above a hot plume head, rather than models that advocate no role for a chemically and thermally distinct plume (e.g., Mutter et al., 1988). From our data alone, we cannot tell if the plume was active in driving plate separation, but we note that magmatic activity was underway in the Southeast Greenland region several million years before the eventual plate break up and separation (e.g., Vogt and Avery, 1974; Saunders et al., 1997; Sinton and Duncan, 1998; Larsen and Saunders, 1998) showing that the thermal anomaly preceded plate fragmentation.

CONCLUSIONS

1. The upper unit drilled at Site 988 at 66°N is a light-REE-enriched basalt that closely resembles tholeiites recovered from Site 407 in the Irminger Basin and Unit 918-1 at 63°N. The basalt has isotopic characteristics similar to those of some Icelandic basalts.

2. The two analyzed units from Site 989 and the six units from Site 990 show isotopic and element diversity indicating that the magmas were variably contaminated by continental crust. Bulk mixing calculations indicate that addition of >5% of continental crust to a primary, light-REE-depleted parental melt will replicate the range of compositions at Sites 989 and 990. The contaminant has characteristics of both Archean granulite and amphibolite facies gneiss with low $^{206}Pb/^{204}Pb$.

3. The primary melts for the lavas at Sites 915, 989, and 990 were probably similar to that recorded by the lavas at Site 918: light-REE depleted, a $^{206}Pb/^{204}Pb$ value of ~18, an εNd value of +8.8, and $^{87}Sr/^{86}Sr$ value of ~0.7030. None of the analyzed lavas from the Southeast Greenland margin has $^{206}Pb/^{204}Pb_{(measured)}$ in excess of 18.3, which is at the low end of the MORB and Icelandic isotope arrays.

4. Although the REE and isotope data do not provide an unequivocal answer to the question of whether the sublithospheric mantle was Icelandic plume or MORB mantle, the relatively high Nb (positive ΔNb) of most of the basalts from Sites 915, 918, 989, and 990 suggests that the source comprised depleted Icelandic mantle. Most of the basalts and picrites from Site 917 appear to have been derived from a normal MORB mantle source, with the exception of periodic extraction from enriched Icelandic mantle during formation of the Site 917 Lower Series basalts.

5. At the time of emplacement of the lavas at Sites 915, 989, and 990, the lithosphere was severely attenuated, allowing extensive decompression melting (to a degree similar to that seen on the main SDRS at Site 918), and probably in a fully developed rift zone (see Larsen et al., Chap. 7, this volume). That this rift zone was not entirely oceanic is clearly shown by the crustal contamination recorded in many of the lavas at Sites 915, 989, and 990.

ACKNOWLEDGMENTS

We thank John Lassiter and David Peate for their constructive reviews. Godfrey Fitton, Pamela Kempton, and Andrew Saunders acknowledge support by the Natural Environment Research Council, United Kingdom, for ODP-related studies in the North Atlantic area (GST/02/673 and GST/02/1227).

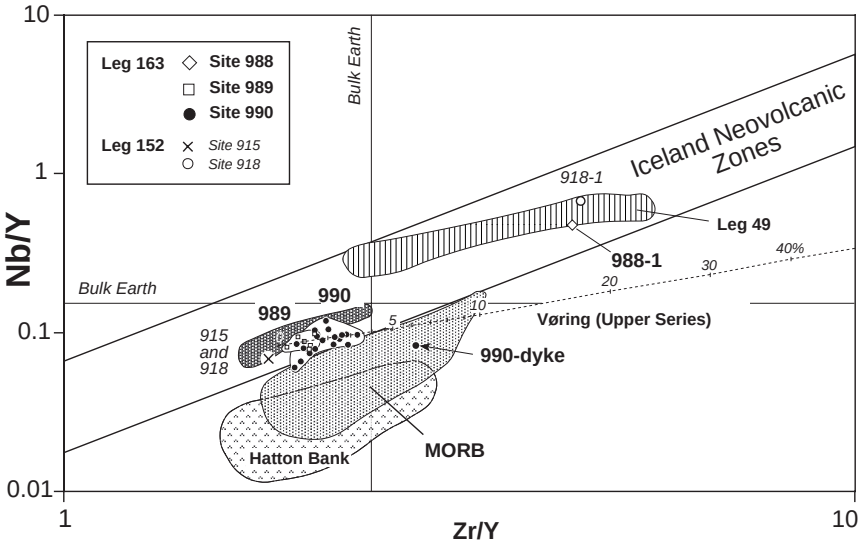

Figure 12. Leg 163 basalts and selected lavas from the North Atlantic igneous province plotted on a Zr/Y vs. Nb/Y diagram. The two diagonal parallel lines outline the array defined by Fitton et al. (1997, 1998b) for all basalts from the neovolcanic zones on Iceland. MORBs plot below this array, thus distinguishing light-REE-depleted Icelandic basalts from MORB. The dashed line shows a mixing trajectory between a basaltic end-member (average Site 918 lava with additional 30% olivine, 39 ppm Zr, 21 ppm Y, and 1.8 ppm Nb) and a crustal contaminant (gneiss GGU324721 from Blichert-Toft et al., 1995 with 333 ppm Zr, 16 ppm Y, and 11.4 ppm Nb). Data sources for Leg 163 are this paper and Larsen et al. (Chap. 7, this volume); MORB, Saunders (unpubl. data); Hatton Bank, Brodie and Fitton (1998); Leg 49 (Sites 407, 408, and 409), Tarney et al. (1979); Vøring Plateau (Site 642, Upper Series lavas), Viereck et al. (1989). Bulk Earth-normalizing values from McDonough and Sun (1995).

REFERENCES

Blichert-Toft, J., Rosing, M.T., Lesher, C.E., and Chauvel, C., 1995. Geochemical constraints on the origin of the late Archean Skjoldungen alkaline igneous province, SE Greenland. *J. Petrol.*, 36:515–561.

Brodie, J.A., and Fitton, J.G., 1998. *Data Report*: Composition of basaltic lavas from the seaward-dipping reflector sequence recovered during Deep Sea Drilling Project Leg 81 (Hatton Bank). *In* Saunders, A.D., Larsen, H.C., and Wise, S.W., Jr. (Eds.), *Proc. ODP, Sci. Results*, 152: College Station, TX (Ocean Drilling Program), 431–435.

Campbell, I.H., and Griffiths, R.W., 1990. Implications of mantle plume structure for the evolution of flood basalts. *Earth Planet. Sci. Lett.*, 99:79–93.

Cohen, R.S., Evensen, N.M., Hamilton, P.J., and O'Nions, R.K., 1980. U-Pb, Sm-Nd and Rb-Sr systematics of mid-ocean ridge basalt glasses. *Nature*, 283:149–153.

Cohen, R.S., and O'Nions, R.K., 1982. The lead, neodymium and strontium isotopic structure of ocean ridge basalts. *J. Petrol.*, 23:299–324.

Demant, A., 1998. Mineral chemistry of volcanic sequences from Hole 917A, southeast Greenland Margin. *In* Saunders, A.D., Larsen, H.C., and Wise, S.W., Jr. (Eds.), *Proc. ODP, Sci. Results*, 152: College Station, TX (Ocean Drilling Program), 403–416.

Dickin, A.P., 1981. Isotope geochemistry of Tertiary igneous rocks from the Isle of Skye, N. W. Scotland. *J. Petrol.*, 22:155–189.

Duncan, R.A., Larsen, H.C., Allan, J.F., et al., 1996. *Proc. ODP, Init. Repts.*, 163: College Station, TX (Ocean Drilling Program).

Eldholm, O., Thiede, J., Taylor, E., et al., 1987. *Proc. ODP, Init. Repts.*, 104: College Station, TX (Ocean Drilling Program).

Elliott, T.R., Hawkesworth, C.J., and Grönvold, K., 1991. Dynamic melting of the Iceland plume. *Nature*, 351:201–206.

Fitton, J.G., Hardarson, B.S., Ellam, R.M., Rogers, G., 1998a. Sr-, Nd-, and Pb-isotopic composition of volcanic rocks from the southeast Greenland Margin at 63°N: temporal variation in crustal contamination during continental breakup. *In* Saunders, A.D., Larsen, H.C., and Wise, S.W., Jr. (Eds.), *Proc. ODP, Sci. Results*, 152: College Station, TX (Ocean Drilling Program), 351–357.

Fitton, J.G., Saunders, A.D., Larsen, L.M., Hardarson, B.S., and Norry, M.J., 1998b. Volcanic rocks from the southeast Greenland Margin at 63°N: composition, petrogenesis, and mantle sources. *In* Saunders, A.D., Larsen, H.C., and Wise, S.W., Jr. (Eds.), *Proc. ODP, Sci. Results*, 152: College Station, TX (Ocean Drilling Program), 331–350.

Fitton, J.G., Saunders, A.D., Norry, M.J., Hardarson, B.S., and Taylor, R., 1997. Thermal and chemical structure of the Iceland plume. *Earth Planet. Sci. Lett.*, 153:97–208.

Fram, M.S., Lesher, C.E., and Volpe, A.M., 1998. Mantle melting systematics: transition from continental to oceanic volcanism on the southeast Greenland Margin. *In* Saunders, A.D., Larsen, H.C., and Wise, S.W., Jr. (Eds.), *Proc. ODP, Sci. Results*, 152: College Station, TX (Ocean Drilling Program), 373–386.

Furman, T., Frey, F.A., and Park, K.H., 1991. Chemical constraints on the petrogenesis of mildly alkaline lavas from Vestmannaeyjar, Iceland; the Eldfell (1973) and Surtsey (1963–1967) eruptions. *Contrib. Mineral. Petrol.*, 109:19–37.

Gariépy, C., Ludden, J., and Brooks, C., 1983. Isotopic and trace element constraints on the genesis of the Faeroe lava pile. *Earth Planet. Sci. Lett.*, 63:257–272.

Hart, S.R., Schilling, J.-G., and Powell, J.L., 1973. Basalts from Iceland and along the Reykjanes Ridge: Sr isotope geochemistry. *Nature*, 246:104–107.

Hémond, C., Arndt, N.T., and Hofmann, A.W., 1993. The heterogeneous Iceland plume: Nd-Sr-O and trace element constraints. *J. Geophys. Res.*, 98:15833–15850.

Hofmann, A.W., Jochum, K.P., Seufert, M., and White, W.M., 1986. Nb and Pb in oceanic basalts: new constraints on mantle evolution. *Earth Planet. Sci. Lett.*, 79:33–45.

Ito, E., White, W.M., and Göpel, C., 1987. The O, Sr, Nd and Pb isotope geochemistry of MORB. *Chem. Geol.*, 62:157–176.

Joron, J.L., Bougault, H., Maury, R.C., Bohn, M., and Desprairies, A., 1984. Strongly depleted tholeiites from the Rockall Plateau margin, North Atlantic: geochemistry and mineralogy. *In* Roberts, D.G., Schnitker, D., et al., *Init. Repts. DSDP*, 81: Washington (U.S. Govt. Printing Office), 783–794.

Kalsbeek, F., Austrheim, H., Bridgwater, D., Hansen, B.T., Pedersen, S., and Taylor, P.N., 1993. Geochronology of Archaean and Proterozoic events in the Ammassalik area, South-East Greenland, and comparisons with the Lewisian of Scotland and the Nagssugtoqidian of West Greenland. *Precambrian Res.*, 62:239–270.

Kerr, A.C., Saunders, A.D., Hards, V.L., Tarney, J., and Berry, N.H., 1995. Depleted mantle plume geochemical signatures: no paradox for plume theories. *Geology*, 23:843–846.

Larsen, H.C., Dahl-Jensen, T., and Hopper, J.R., 1998. Crustal structure along the Leg 152 drilling transect. *In* Saunders, A.D., Larsen, H.C., and Wise, S.W., Jr. (Eds.), *Proc. ODP, Sci. Results*, 152: College Station, TX (Ocean Drilling Program), 463–475.

Larsen, H.C., and Jakobsdóttir, S., 1988. Distribution, crustal properties and significance of seawards-dipping sub-basement reflectors off E Greenland. *In* Morton, A.C., and Parson, L.M. (Eds.), *Early Tertiary Volcanism and the Opening of the NE Atlantic*. Geol. Soc. Spec. Publ. London, 39:95–114.

Larsen, H.C., and Saunders, A.D., 1998. Tectonism and volcanism at the southeast Greenland rifted margin: a record of plume impact and later continental rupture. *In* Saunders, A.D., Larsen, H.C., and Wise, S.W., Jr.

(Eds.), *Proc. ODP, Sci. Results*, 152: College Station, TX (Ocean Drilling Program), 503–533.

Larsen, H.C., Saunders, A.D., Clift, P.D., et al., 1994. *Proc. ODP, Init. Repts.*, 152: College Station, TX (Ocean Drilling Program).

Larsen, L.M., Fitton, J.G., and Fram, M.S., 1998. Volcanic rocks of the southeast Greenland Margin in comparison with other parts of the North Atlantic tertiary igneous province. *In* Saunders, A.D., Larsen, H.C., and Wise, S.W., Jr. (Eds.), *Proc. ODP, Sci. Results*, 152: College Station, TX (Ocean Drilling Program), 315–330.

Lawver, L.A., and Müller, R.D., 1994. Iceland hotspot track. *Geology*, 22:311–314.

Leeman, W.P., Dasch, E.J., and Kays, M.A., 1976. $^{207}Pb/^{206}Pb$ whole-rock age of gneisses from the Kangerdlugssuaq area, eastern Greenland. *Nature*, 263:469–471.

Luyendyk, B.P., Cann, J.R., et al., 1979. *Init. Repts. DSDP*, 49: Washington (U.S. Govt. Printing Office).

Macintyre, R.M., and Hamilton, P.J., 1984. Isotopic geochemistry of lavas from Sites 553 and 555. *In* Roberts, D.G., Schnitker, D., et al., *Init. Repts. DSDP*, 81: Washington (U.S. Govt. Printing Office), 775–781.

Mattinson, J.M., 1979. Lead isotope studies of basalts from IPOD Leg 49. *In* Luyendyk, B.P., Cann, J.R., et al., *Init. Repts. DSDP*, 49: Washington (U.S. Govt. Printing Office), 721–726.

McDonough, W.F., and Sun, S.-S., 1995. The composition of the Earth. *Chem. Geol.*, 120:223–253.

Merriman, R.J., Taylor, P.N., and Morton, A.C., 1988. Petrochemistry and isotope geochemistry of early Palaeogene basalts forming the dipping reflector sequence SW of Rockall Plateau, NE Atlantic. *In* Morton, A.C., and Parson, L.M. (Eds.), *Early Tertiary Volcanism and the Opening of the NE Atlantic*. Geol. Soc. Spec. Publ. London, 39:123–134.

Miller, J.A., Matthews, D.H., and Roberts, D.G., 1973. Rocks of Grenville age from Rockall Bank. *Nature*, 246:61.

Morton, A.C., and Taylor, P.N., 1987. Lead isotope evidence for the structure of the Rockall dipping-reflector passive margin. *Nature*, 326:381–383.

Mutter, J.C., Buck, W.R., and Zehnder, C.M., 1988. Convective partial melting, 1. A model for the formation of thick basaltic sequences during the initiation of spreading. *J. Geophys. Res.*, 93:1031–1048.

Nakamura, N., 1974. Determination of REE, Ba, Fe, Mg, Na, and K in carbonaceous and ordinary chondrites. *Geochim. Cosmochim. Acta*, 38:757–776.

Richards, M.A., Duncan, R.A., and Courtillot, V.E., 1989. Flood basalts and hot-spot tracks: plume heads and tails. *Science*, 246:103–107.

Saunders, A.D., Fitton, J.G., Kerr, A.C., Norry, M.J., and Kent, R.W., 1997. The North Atlantic igneous province. *In* Mahoney, J. J., and Coffin, M. F. (Eds.), *Large Igneous Provinces.* Geophys. Monogr., Am. Geophys. Union, 45–94.

Saunders, A.D., Larsen, H.C., and Fitton, J.G., 1998. Magmatic development of the southeast Greenland Margin and evolution of the Iceland Plume: geochemical constraints from Leg 152. *In* Saunders, A.D., Larsen, H.C., and Wise, S.W., Jr. (Eds.), *Proc. ODP, Sci. Results*, 152: College Station, TX (Ocean Drilling Program), 479–501.

Schilling, J.-G., 1973. Iceland mantle plume: geochemical study of Reykjanes Ridge. *Nature*, 242:565–571.

Sheraton, J.W., Skinner, A.C., and Tarney, J., 1973. The geochemistry of the Scourian gneisses of the Assynt district. *In* Park, R.G., and Tarney, J. (Eds.), *The Early Precambrian of Scotland and Related Rocks of Greenland.* Univ. of Keele, UK, 13–30.

Sinton, C.W., and Duncan, R.A., 1998. ^{40}Ar-^{39}Ar ages of lavas from the southeast Greenland Margin, ODP Leg 152, and the Rockall Plateau, DSDP Leg 81. *In* Saunders, A.D., Larsen, H.C., and Wise, S.W., Jr. (Eds.), *Proc. ODP, Sci. Results*, 152: College Station, TX (Ocean Drilling Program), 387–402.

Sun, S.-S., and Jahn, B., 1975. Lead and strontium isotopes in post-glacial basalts from Iceland. *Nature*, 255:527–530.

Tarney, J., Saunders, A.D., Weaver, S.D., Donnellan, N.C.B., and Hendry, G.L., 1979. Minor element geochemistry of basalts from Leg 49, North Atlantic Ocean. *In* Luyendyk, B.P., Cann, J.R., et al., *Init. Repts. DSDP*, 49: Washington (U.S. Govt. Printing Office), 657–691.

Taylor, P.N., Kalsbeek, F., and Bridgwater, D., 1992. Discrepancies between neodymium, lead and strontium model ages from the Precambrian of southern East Greenland: evidence for a Proterozoic granulite-facies event affecting Archaean gneisses. *Chem. Geol.*, 94:281–291.

Taylor, P.N., and Morton, A.C., 1989. Sr, Nd, and Pb isotope geochemistry of the upper and lower volcanic series at Site 642. *In* Eldholm, O., Thiede, J., Taylor, E., et al., *Proc. ODP, Sci. Results*, 104: College Station, TX (Ocean Drilling Program), 429–435.

Taylor, R.N., Thirlwall, M.F., Murton, B.J., Hilton, D.R., and Gee, M.A.M., 1997. Isotopic constraints on the influence of the Icelandic plume. *Earth Planet. Sci. Lett.*, 148:E1–E8.

Thirlwall, M.F., 1995. Generation of Pb isotopic characteristics of the Iceland plume. *J. Geol. Soc. London*, 152:991–996.

Thirlwall, M.F., Upton, B.G.J., and Jenkins, C., 1994. Interaction between continental lithosphere and the Iceland plume: Sr-Nd-Pb isotope geochemistry of Tertiary basalts, NE Greenland. *J. Petrol.*, 35:839–879.

Thy, P., Lesher, C.E., and Fram, M.S., 1998. Low pressure experimental constraints on the evolution of basaltic lavas from Site 917, southeast Greenland continental margin. *In* Saunders, A.D., Larsen, H.C., and Wise, S.W., Jr. (Eds.), *Proc. ODP, Sci. Results*, 152: College Station, TX (Ocean Drilling Program), 359–372.

Todt, W., Cliff, R.A., Hanser, A., and Hoffmann, A.W., 1993. Re-calibration of NBS lead standards using a ^{202}Pb + Pb double spike. *Terra Abstr.*, 5:396.

Viereck, L.G., Hertogen, J., Parson, L.M., Morton, A.C., Love, D., and Gibson, I.L., 1989. Chemical stratigraphy and petrology of the Vøring Plateau tholeiitic lavas and interlayered volcaniclastic sediments at ODP Hole 642E. *In* Eldholm, O., Thiede, J., Taylor, E., et al., *Proc. ODP, Sci. Results*, 104: College Station, TX (Ocean Drilling Program), 367–396.

Viereck, L.G., Taylor, P.N., Parson, L.M., Morton, A.C., Hertogen, J., Gibson, I.L., and the ODP Leg 104 Scientific Party, 1988. Origin of the Palaeogene Vøring Plateau volcanic sequence. *In* Morton, A.C., and Parson, L.M. (Eds.), *Early Tertiary Volcanism and the Opening of the Northeast Atlantic*. Geol. Soc. Spec. Publ. London, 39:69–83.

Vogt, P.R. and Avery, O.E., 1974. Detailed magnetic surveys in the northeast Atlantic and Labrador Sea. *J. Geophys. Res.*, 79:363–389.

White, R.S., and McKenzie, D., 1989. Magmatism at rift zones: the generation of volcanic continental margins and flood basalts. *J. Geophys. Res.*, 94:7685–7729.

Wood, D.A., Joron, J.L., Treuil, M., Norry, M.J., and Tarney, J., 1979. Elemental and Sr isotope variations in basic lavas from Iceland and the surrounding ocean floor. *Contrib. Mineral. Petrol.*, 70:319–339.

Wood, D.A., Varet, J., Bougaut, H., Corre, O., Joron, J.-L., Treuil, M., Bizouard, H., Norry, M.J., Hawkesworth, C.J., and Roddick, J.C., 1979. The petrology, geochemistry, and mineralogy of North Atlantic basalts: a discussion based on IPOD Leg 49. *In* Luyendyk, B.P., Cann, J.R., et al., *Init. Repts. DSDP*, 49: Washington (U.S. Govt. Printing Office), 597–655.

Date of initial receipt: 5 January 1998
Date of acceptance: 8 July 1998
Ms 163SR-122

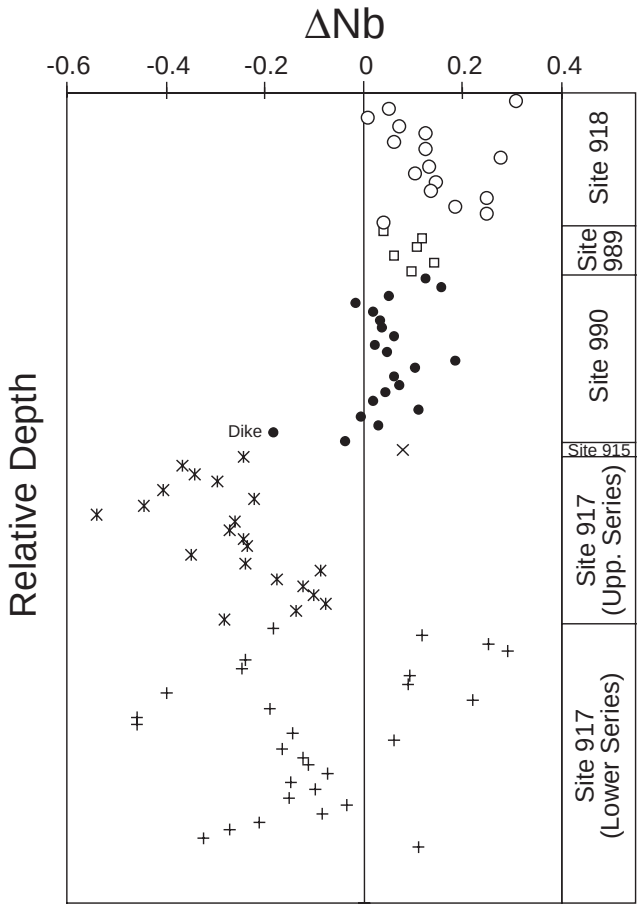

Figure 13. Plot of ΔNb vs. relative depth for basalts recovered from the 63°N transect, Southeast Greenland margin, during Legs 152 and 163. ΔNb reflects the excess or deficiency of Nb, using the lower bound of the Iceland array (Fig. 12) as a reference line: $\Delta Nb = 1.74 + \log(Nb/Y) - 1.92 \cdot \log(Zr/Y)$ (Fitton et al., 1997). Uncontaminated samples with a negative value for ΔNb imply a derivation from the depleted (MORB) upper mantle, whereas samples with positive ΔNb imply a derivation from an Icelandic mantle source. Depth scale is relative (e.g., the Site 917 Middle Series is omitted, as are the gaps between the different sites, and the basalts from Site 990 may be younger than those from Site 989). Data sources for Leg 163 are this paper and Larsen et al. (Chap. 7, this volume); Leg 152, Fitton et al. (1998b).